AD-A246 904

NAVSWC TR 91-460

INFRARED HORIZON DETECTION

BY MONTE S. KAELBERER
RESEARCH AND TECHNOLOGY DEPARTMENT

31 JULY 1991

DTIC
ELECTE
MAR 05 1992
S B D

Approved for public release; distribution is unlimited.

Original containing color plates: All DTIC reproductions will be in black and white

NAVAL SURFACE WARFARE CENTER

Dahlgren, Virginia 22448-5000 • Silver Spring, Maryland 20903-5000

92-05146

NAVSWC TR 91-460

INFRARED HORIZON DETECTION

BY MONTE S. KAELBERER
RESEARCH AND TECHNOLOGY DEPARTMENT

31 JULY 1991

Approved for public release; distribution is unlimited.

NAVAL SURFACE WARFARE CENTER
Dahlgren, Virginia 22448-5000 • Silver Spring, Maryland 20903-5000

FOREWORD

This report examines the sea/sky interface in the 3-5 micron and 8-12 micron regions and studies the efficacy of two algorithms for delineating the optical horizon. The infrared data used in this study was taken with the Infrared Analysis, Measurement, and Modeling Program (IRAMMP) sensor and was collected at two separate test sites: Port Hueneme, California, and Marathon, Florida. Some signal processing methods for horizon detection and horizon contrast measurement are presented along with the performance results of computer simulations exercising the various algorithms against the IRAMMP data. Accompanying meteorological data is used to aid in explaining the varying degrees of contrast exhibited by the database.

Funding for this work was provided by the Surface Launched Weaponry Block's subtask on multi-sensor signal processing which is managed by Mr. Ron Stapleton of the Surface Weapons Technology Branch, F41, Naval Surface Warfare Center, Dahlgren, Virginia. The author wishes to thank Messrs. Karl Krueger and Russ Wiss for their direction, Darren Parker for his compilation of the meteorological data, with special thanks to Mr. John Barnett for his help and guidance during this study.

Approved by:

C. W. LARSON, Head
Physics Technology Division

CONTENTS

Section		Page
1	INTRODUCTION	1
2	IRAMMP SENSOR	3
3	TEST SITES	5
4	HORIZON SCENES	7
5	HORIZON TYPES	11
6	HORIZON DETECTION	13
7	CONTRAST MEASUREMENT	17
8	ANALYSIS OF CONTRAST	19
9	CONCLUSIONS AND RECOMMENDATIONS	23
	DISTRIBUTION	(1)

DTIC COPY INSPECTED

Accession For
NTIS GRA&I ☑
DTIC TAB ☐
Unannounced ☐
Justification
By
Distribution/
Availability Codes
Dist | Avail and/or Special
A-1

ILLUSTRATIONS

Figure		Page
1	PORT HUENEME TEST SITE	25
2	SCENE 0162-13, MIDWAVE FILTER 5 . .	26
3	SCENE 0162-14, MIDWAVE FILTER 6 . .	27
4	SCENE 0162-15, MIDWAVE FILTER 7 . .	28
5	IMAGE, SCENE 0162-13, MIDWAVE FILTER 5 .	29
6	IMAGE, SCENE 0162-15, MIDWAVE FILTER 7 .	29
7	POSITIVE CONTRAST, SCENE 0157-01, LONGWAVE	31
8	SAMPLES 500-800, SCENE 0157-01, LONGWAVE	32
9	NEGATIVE CONTRAST, SCENE 0200-24, MIDWAVE .	33
10	IMAGE, SCENE 0157-01, LONGWAVE . .	35
11	IMAGE, SCENE 0200-24, MIDWAVE . . .	35
12	SYMMETRIC CONTRAST, 5 SCAN AVERAGE, SCENE 0195-09, MIDWAVE . . .	37
13	SYMMETRIC CONTRAST, 5 SCAN AVERAGE, SCENE 0195-09, LONGWAVE . . .	38
14	IMAGE, SCENE 0195-09, MIDWAVE, 5 SCAN AVERAGE	39
15	IMAGE, SCENE 0195-09, LONGWAVE, 5 SCAN AVERAGE	39
16	ZERO-CROSSING METHOD	41
17	SCENE 0157-01, MIDWAVE	42
18	IMAGE, SCENE 0157-01, MIDWAVE . . .	43
19	SAMPLES 600-700, SCENE 0157-01, MIDWAVE .	45
20	FIVE SAMPLE SMOOTHING, SAMPLES 600-700, SCENE 0157-01, MIDWAVE . . .	46
21	ELEVEN SAMPLE SMOOTHING, SAMPLES 600-700, SCENE 0157-01, MIDWAVE . . .	47
22	PREDICTION METHOD	48
23	SAMPLE CONTRAST, LONGWAVE SCENES . .	49
24	SAMPLE CONTRAST, MIDWAVE SCENES . .	50

TABLES

Table		Page
1	HORIZON SCENES PROCESSED . . .	51
2	ZERO-CROSSING, HORIZON DETECTION, SCENE 0157-01, MIDWAVE . . .	52
3	ZERO-CROSSING DETECTION ON TEMPORALLY AVERAGED SCANS OF SCENE 0195-09 . .	52
4	PREDICTION METHOD ON LONGWAVE AND MIDWAVE SCENE 0157-01	53
5	RESULTS OF RADIANCE CONTRAST AND SAMPLE CONTRAST METHODS . . .	54
6	METEOROLOGICAL CONDITIONS FOR EACH SCENE .	55
7	MIDWAVE SORTED BY RADIANCE CONTRAST . .	56
8	LONGWAVE SORTED BY RADIANCE CONTRAST .	58
9	RADIANCE CONTRAST IN NEI UNITS AND CELSIUS DEGREES	60

SECTION 1

INTRODUCTION

Low flying threats often require that they be detected as soon as they cross the horizon in order to be countered successfully. Knowledge of the location of the infrared (IR) horizon then becomes an important reference area which can be searched for targets. Infrared sensors, which are designed for detection of targets near the horizon, may have a vertical field of view of on the order of 15 to 30 milliradians, along with a vertical resolution of approximately 100 microradians. Stabilization for such a sensor will be difficult but appears to be achievable with current technologies. However, even with stabilized platforms, refractive effects may cause the apparent location of the optical horizon to shift by as much as 1 to 2 milliradians because of changes in the air/sea temperature difference. If the optical horizon can be determined to within the accuracy of the sensor, operation of such a horizon surveillance IR sensor can be optimized to detect targets as soon as they appear above the horizon.

This report documents the performance of signal processing algorithms for horizon extraction using data taken with the Infrared Analysis, Measurement, and Modeling Program (IRAMMP) sensor at Port Hueneme, California, and Marathon, Florida, and includes data from both the 2-5 micron (midwave) and 8-12 micron (longwave) atmospheric windows. In Sections 2, 3, and 4, the IRAMMP sensor, the test sites, and the scenes chosen for analysis will be briefly described. In Sections 5 and 6, three horizon types will be described and two horizon detection methods will be explained along with the performance results of computer simulations exercised on the data. A metric for measuring the horizon contrast is then introduced and used to compare the midwave and longwave. Finally, the accompanying meteorological data will be incorporated into the analyses to assist in examining what parameters influenced the contrast.

SECTION 2

IRAMMP SENSOR

The IRAMMP sensor was built by Raytheon and is owned and operated by the Naval Surface Warfare Center (NAVSWC) in Silver Spring, Maryland. It is an IR, dual band, radiometric sensor designed to take background radiance data in the midwave band of 2-5 microns and longwave band of 8-12 microns. A filter wheel for the midwave detectors contains seven selectable sub-bands. The sensor uses an indium antimonide linear array of 120 detectors for the midwave band and a mercury cadmium telluride linear array of the same size for the longwave band. The noise equivalent irradiance (NEI) in the midwave band is 2.6×10^{-14} W cm^{-2} and 2.6×10^{-13} W cm^{-2} for the longwave.

The instantaneous field of view (IFOV) of one detector is 0.23 milliradians in azimuth and elevation. In the normal operating mode, the total field of view is 5.6 degrees in azimuth by 1.6 degrees in elevation with a scan speed of 34 degrees per second. More than three scans per second are taken for the 5.6 degree field of view. The sampling rate for each detector is 8800 samples per second. This rate will sample a point source over three times per IFOV in the scanning direction. In the non-scanned direction, parallel to the detector array, a point source is sampled once per IFOV. The sensor has a scan-to-scan registration of 0.28 IFOV, a color-to-color registration of 0.27 IFOV, and a dynamic range of 84 dB.

Data is taken simultaneously in each band, digitized, and recorded on a 28 track Fairchild-Weston high density, digital recorder. The high density tapes are reduced by Questech, Inc. The data reduction calibrates and formats the raw data for placement on computer compatible tapes.

SECTION 3

TEST SITES

IRAMMP measurements were conducted at Port Hueneme, California, in support of the operational testing of the AN/SAR-8 IR system at the Naval Surface Weapons Systems Engineering Station under the direction of Joe Niederst. The IRAMMP data collection took place over the period 1 June to 19 June 1990. The sensor was located on a roof at a height of about 9.1 meters above sea level. The coast faced south, and the sea/sky horizon was partially obstructed by islands, buildings, and utility poles. The islands Anacapa and Santa Cruz covered the azimuths from 224-236 degrees and 244-256 degrees, respectively. The location of the islands and an oil rig (small circle), with respect to Port Hueneme, are shown in Figure 1.

There were a number of meteorological measurements taken at different locations and at different times during the field test. Hourly measurements of temperature, relative humidity, and wind direction and speed were taken on the rooftop alongside the IRAMMP sensor. Radiosonde data, with the same type of measurements, was taken at Point Mugu and San Nicholas Island which are located 8 miles south southeast and 60 miles south southwest, respectively. At most, three balloons were released daily at approximate times of 0700, 1100, and 2200 hours. On some days a plane was available which had meteorological equipment on board and could take measurements along the line of sight and at different altitudes. Dr. Doug Jensen of the Naval Ocean Systems Center (NOSC), San Diego, California, supervised the operation of the plane and entered the test range once a day to make several passes over the area of interest. His data included extinction coefficients which were useful in comparing the variance of the visibility during the field test. Water and air temperatures at sea level were taken by a buoy located near San Nicholas Island.

The meteorological data was useful in comparing weather conditions for different days of the test, but it was not taken sufficiently often to offer help for different times within the same day. Also, the location at which some of the data was collected was far from the actual area of interest, for example, the radiosonde data. The rooftop measurements were made hourly but reflect land-based conditions rather than maritime conditions. The data collected by Dr. Jensen was along the line of sight to the horizon, but the time at which it was taken was usually quite different from the time at which horizon data was taken. Therefore, the weather conditions reported should be taken as an indication of the general weather pattern for that time but not as a precise measurement of the conditions along the line of sight.

The second test site was located at Marathon, Florida. The sensor was placed on the balcony of a tenth floor condominium at a height of 28 meters

above sea level. Data was taken from 5 July to 19 July 1990, from a balcony facing south and also through a window facing east. The field test was directed by the Naval Research Laboratory, and its purpose was to investigate horizon phenomenology. An IR source on a boat, which traveled out towards the horizon, was used for the field test. Unlike Port Hueneme, there were no obstructions in the line of sight to the horizon.

Meteorological support was provided by Dr. Jensen using a plane to record data along radial paths to and from the condominium and along spiral paths through different altitudes. Radon counter measurements were collected, but will not be used in this report.

SECTION 4

HORIZON SCENES

Many scenes are available from the two test sites. The scenes differ mainly in their geographical location, azimuth, midwave bandpass, scanning direction, and time of day. A scene is a collection or series of scans which are taken consecutively for a period of time. A scan is the image created by one pass of the scanning mirror over the linear array. Typically this produces a 1400 by 120 element data array after the analog to digital conversion (1400 samples of each of the 120 detectors). A scan produces an image of the 5.6 degree by 1.6 degree field of view mentioned earlier in this report. A sample is a single value collected from a detector by the analog to digital converter. The sensor normally scans in the azimuth direction (the 1400 samples), and this is referred to as horizontal scanning. However, the sensor can be tipped on its side so that it scans in the elevation direction for vertical scanning. In this mode the total field of view is rotated 90 degrees such that the sensor scans 5.6 degrees in elevation with 1.6 degrees in azimuth. Horizontal scanning has three samples per IFOV in the azimuth direction and one sample per IFOV in the elevation direction while vertical scanning is vice versa.

At Port Hueneme there were almost 200 scenes of the sea/sky horizon while at Marathon the total was around 140 scenes. Selecting a subset from this large set of scenes was accomplished by considering the following two factors. First, for scenes less than several hours apart, the contrast did not change enough to warrant study so only one representative scene was selected. This was a greater factor in the selection process of Marathon scenes than in the selection process of Port Hueneme scenes. However, this restriction was relaxed during the sunrise and sunset hours because of fast changing contrast conditions.

The second factor restricted the choice of midwave sub-bands to filter number 5 because only filter 5 was used at both test sites and the data taken was not as subject to quantization effects as in the other bands. At Port Hueneme, filters 5, 6, and 7 were used while at Marathon only filters 5 and 6 were used. Filters 5, 6, and 7 of the filter wheel have full width, half maximum bandpasses of 3.8-4.9 microns, 3.9-4.1 microns, and 4.4-5.0 microns, respectively. In the longwave, the bandpass was 7.8-11.9 microns. Some preliminary investigation into low contrast scenes showed the quantization effects from the digitization of the sensor analog outputs were worse for filters 6 and 7 than they were for filter 5. This is reasonable since filters 6 and 7 are narrower bandpasses and thus transmit less energy. The contrast or variance in some scenes was low enough so that strings of several hundred samples all fell within several quantization levels. As an illustration of the quantization for each filter, Figures 2, 3, and 4 are filters 5, 6, and 7,

respectively. Each figure is a graph of detector (or channel) 21 and is at the same azimuth and time as the others. Figures 2, 3, and 4 are examples from scenes 0162-13, 0162-14, and 0162-15 of vertical scanning. Samples 600-1400 are sky samples while samples 200-600 are water samples. A jetty of sand and rocks interrupts the water at samples 0-200 and these radiance values have been truncated. The peaks at samples 700, 1000, and 1300 are caused by guy wires to a radio tower. Notice filter 7 closely resembles filter 5 in radiance range but, since filters 5 and 6 were the only filters used at both Port Hueneme and Marathon, filter 5 was chosen for this report.

Figures 5 and 6 are color images of scenes 0162-13, filter 5, and 0162-15, filter 7, respectively. These images, along with the others in this report, were created using a false color scheme of four shades of black, four shades of blue, four shades of green, three shades of red, and one white. The colors in order of increasing radiance are black, blue, green, red, and white. The color scheme is non-linear in the sense that going from black to blue may not equal the radiance in going from blue to green. The non-linear scale was used because it produced images which used the colors more equally and thus enhanced the contrast within the image. The images were included because they show the overall IR contrast between the horizon and the other IR sources in the scene. All the images shown in this report are of vertical scans with a restricted field of view of 2.4 degrees in elevation by 1.5 degrees in azimuth. The elevation angle increases (sample number increases) as you move from left to right in the image. Figures 5 and 6 clearly show the oil rig (middle elevation area) and the three diagonal guy wires which pass through the water and the sky. At the right-most azimuth in both figures is a strip of red and white; this was caused by the edge of a light pole that was just coming into the field of view. The horizontal wires are close to the horizon and show up as strips of green in Figure 5 and strips of green and light blue in Figure 6. A rod separating the two horizontal wires appears as a white bar at the right end of the wires.

A total of 31 scenes from Port Hueneme and 11 scenes from Marathon were analyzed. Table 1 lists the scenes selected for processing in this report. All scenes contained the midwave and the longwave except scenes 0198-13, 0200-11, 0200-14, 0200-17, and 0200-22 which had only the longwave. The scene column describes the year, Julian day, and scene of that day. For example, the "0" in "0152" stands for 1990 and "152" is the Julian day. The number after the hyphen is the scene number. For reference, day 0152 is June 1, 1990, and day 0186 is July 5, 1990. These dates mark the first days from Port Hueneme and Marathon, respectively. The sensor azimuth column refers to the azimuth line of sight of the sensor from true north, and the time is the time at which the data was taken (Pacific Daylight Savings Time for Port Hueneme and Eastern Daylight Savings Time for Marathon).

The Port Hueneme azimuths of Table 1 fall into two general areas. Those around 223 degrees have Anacapa Island in the right quarter of the scene. Anacapa is the only obstruction at this azimuth. The majority of azimuths are around 240 degrees. While viewing at this azimuth had obstructions such as diagonal guy wires, horizontal electrical cables, a light pole, and an oil rig, only the horizontal cables caused any problems. They were 10 to 30 samples away from the horizon, and care was taken to avoid their influence on the calculations. The Marathon scenes had no obstructions.

The Marathon and Port Hueneme sites had different weather conditions and different sensor heights. This caused a gap between the Marathon horizon contrast and the Port Hueneme contrast. The evaluation of factors such as the extinction coefficient becomes more difficult to compare between sites in this case, but the separation does broaden the available horizon scene database by showing the dependence of horizon contrast on path length and overall weather conditions. For the sensor height of 9.1 meters at Port Hueneme, the geometric horizon is 11 kilometers, while at Marathon the height of 28.0 meters gives 18 kilometers. The near doubling of the atmospheric path plus the warmer, more humid, climate at Marathon produced the separation of contrast between Port Hueneme and Marathon. Of the scenes analyzed, those with the lowest contrast were typically from Marathon.

SECTION 5

HORIZON TYPES

Three shapes or types of horizon contrast were observed in the data. The most common was what will be called positive contrast. For this horizon type, sea radiance was less than the sky radiance and, thus, there was an increase in radiance with increasing sample number for vertical scans (or decreasing channel number for horizontal scans). Figure 7 is a typical example of positive contrast. It is a longwave scene of day 0157-01. The diagonal wires are visible as the bumps between samples 700-1400; the horizontal wires show up as one bump around sample 645 with the horizon occurring just after the bump. Figure 8 expands the horizon area of Figure 8 between samples 500 and 800. The horizontal wire bumps are now clear as is the first diagonal wire bump.

The next most common type of horizon contrast observed in the data set was negative contrast. For this type the sea radiance was greater than the sky radiance at the horizon. Figure 9 shows the negative contrast from midwave scene 0200-24. This was a Marathon scene and so it shows only sea and sky with no obstructions. The negative contrast was caused by sun glint and will be discussed later in this report. The horizon occurs at approximately sample 590 with the glint between samples 0-590 and the sky between samples 590-1400. Figure 10 is a color image of scene 0157-01 in the longwave and contains the three guy wires, oil rig, and light pole as seen before in Figures 5 and 6. The two horizontal wires are barely discernible along the horizon, and the tops of two fence posts are visible along the lowest elevation. Figure 11 is a color image of scene 0200-24 in the midwave. The sun glint is clearly visible and produced a sharp break between the sky and the water. The structure in the sky is a cloud.

The third type of contrast is symmetric and occurs when the sky and water radiance values form a symmetric peak about the horizon. Figure 12 is an example of symmetric contrast and shows five midwave scans from Marathon, scene 0195-09, that have been averaged together to improve the contrast. There are at least three sharp changes in the graph which suggest a possible horizon occurrence: samples 500, 800, and 875. Figure 13 shows the same five scans averaged together in the longwave and clearly shows the horizon at sample 875. This is an example of how temporal averaging and comparisons between the midwave and longwave can help locate the horizon area. Even though the horizon position is known, the midwave and longwave contrast for this scene cannot be defined as either positive or negative because the sky radiance decreases at the same rate as the water radiance. Figures 14 and 15 are the midwave and longwave color images from scene 0195-09, and each was created by averaging five scans from the scene together. Even after the averaging, the horizon location in the images is unclear in both bands. The

double peak shown in Figure 12 is evident in Figure 14 as the two white band areas. There is some noise present in the center of the image along the elevation. Since it is periodic, it is believed to be electromagnetic interference. It is typically less than five NEI and will show up on low contrast scenes more than it will on high contrast scenes.

SECTION 6

HORIZON DETECTION

Initially the types of horizon contrast were chosen by making a graph of a channel and picking the horizon area by eye. This type of qualitative analysis led to the definition of positive, negative, and symmetric contrast types. The next step was to develop a process which would automatically pick out areas that "looked" like a possible horizon transition. Various statistical methods (averages, standard deviations) were tried, but they were either too sensitive and returned detections for changes in radiance caused by noise, or not sensitive enough and did not detect the horizon. Eventually two methods, both using a linear least squares fit (LLSF), were developed which show promise as a horizon detector. The first was very useful in locating the general area of the horizon and came within several samples of the horizon sample. The second was more sensitive and in high contrast scenes was able to come within plus or minus one sample of the horizon sample. In this section the following two methods were used only on vertical scans. In Section 7 the methods were modified to apply also to horizonal scans.

The first method took advantage of the typically decreasing radiance of the sky with increasing elevation (increasing sample number). Since the majority of scenes were of the positive contrast type, the slope of a LLSF approaching the horizon from the water side would be positive but, once over the horizon, the slope would become negative. The algorithm to detect the horizon performed a linear least squares fit on a window of N samples and recorded the slope. The window was then moved one sample to the right and the slope recalculated. This process was repeated across the entire channel, and any areas at which the slope went from positive to negative was called a zero-crossing. All areas which fit this criteria are potential detections of the horizon. Figure 16 is a graphical representation of the zero-crossing method. For those scenes in which a horizon sample (the last water sample before sky samples) could be picked by eye, this method came within several samples of the one chosen. For those scenes in which a single horizon sample could not be chosen (like the scene in Figure 12 with severe quantization), this method would produce a single sample which could be compared to other channels and scans.

As an example, Figure 17 is an illustration of how complicated the area around the horizon can be. It is of midwave scene 0157-01, channel 21, and is the analog to Figure 7 which was shown earlier. The horizon is around samples 640 to 750. Notice that radiance values above 1.1 W m^{-2} sr^{-1} have been truncated in Figure 17, and this truncation has made the quantization in this scene more evident. The sky radiance increases between samples 800 to 900 because a temperature inversion is present in the atmosphere. In a scene like this, the wires (samples 640, 750, 1075, and 1375) are helpful because they

act as reference points. The horizon must be between samples 640 and 750 because the horizontal wires are below the horizon and the diagonal wires are above the horizon. Figure 18 is a color image of scene 0157-01 in the midwave. Notice the fence at the lowest elevation in which even the barbed wire is visible. The rod that holds the two horizontal wires apart is visible as a white bar at about the middle elevation. Figure 19 is a zoom of Figure 17 around the horizon area with each sample connected by a line. The two peaks caused by the horizontal wires are now visible starting at sample 640. This scene has almost all the undesirable qualities possible for the dataset of this report and using the zero-crossing method on this scene will be a good illustration of what the zero-crossing, horizon detection method can do.

The results of using this zero-crossing method on Figure 17 are shown in Table 2. Three window widths of 20, 40, and 60 samples are used for the LLSF. The total detections column shows the number of detections for samples 0-1400, and column 3 shows the location of detections occurring between samples 600-700 (the horizon area). Using Figure 19, the horizon by eye seems to be around sample 659. All three sample widths have detections in this area as well as a detection at sample 630 which is caused by the wires. The third column shows what you would expect: the total number of detections decreases with increasing sample width because smaller sample widths are more susceptible to short peaks in the data such as the wires. However, as the window width is increased, the detection sample moves farther from the chosen horizon sample of 659; thus larger windows may not perform as well as smaller windows. For the scenes used in this report a sample width of 40 was chosen as a good compromise between decreasing the number of false detections and still maintaining the horizon detection accuracy.

Several things can be done to reduce the false alarms or detections caused by sharp peaks and edges other than the horizon. For example, the data can be smoothed with a boxcar average before the zero-crossing check is applied. Channel 21 of scene 0157-01 was smoothed using a five sample boxcar average, and samples 600-700 are plotted in Figure 20 where each sample is connected by a line. The unsmoothed data was shown in Figure 19. Figure 21 shows the same data smoothed with an 11 sample average. Notice the two peaks of the horizontal wires have now merged into one. This is typical and demonstrates how an edge could be lost if the window size is too large. The results of using a zero-crossing detection method on the smoothed data is shown in the bottom half of Table 2. A smoothing of five samples succeeded in reducing the number of false alarms without affecting the horizon sample detection of 660 and, while a smoothing of 11 samples does further reduce the number of false alarms, it starts to affect the horizon sample resolution.

For those scenes where quantization effects prevent the resolution of the horizon sample to within a desired accuracy, temporal averaging can reduce the variance of the data and bring out features such as edges and peaks. This has already been shown in Figures 12 and 13 in which five consecutive scans were averaged together. For both bands of scene 0195-09, temporal averages of 10, 20, and 30 scans were done, and the zero-crossing method approach was used on each average. The results (in Table 3) show an LLSF with a 20 sample width that will decrease the number of false alarms to about a 20 scan average after which the relative gains are small. For an LLSF of 40 samples, the result is

different. After 10 scans have been averaged, little or no reduction in the number of false alarms is produced. The explanation is related to the reduction of the standard deviation caused by the temporal averaging. After 10 to 20 scans have been averaged, the variance of the data has reached its lower limit, and there are no more noise peaks to be smoothed out to reduce false alarms. Temporal averaging of more than five scans was done only on scene 0195-09 because the additional scans needed for other scenes were not immediately available.

In the above process the horizon detections were found for only one channel but, by comparing the detections in one channel to those in other channels, a reduction in false alarms should result. The process is similar to taking the set of detections in channel one and logically ANDing them with the next channel. The resultant set can be compared with the next channel and so on until only one detection is left or channel 120 is reached. This assumes there are no other horizontal lines or edges in the scene and the horizon stays perpendicular to the vertical scan direction. Neither of the conditions was met ideally, but the problems could be easily handled. For example, if the horizontal wires are in the scene, the detections they cause in each channel can be ignored. If the sensor is not level, the horizon will not be perpendicular to the vertical scan. Scenes in this report had a typical drift of 20 samples between the horizon detection in detector 1 and detector 120. This problem was overcome by comparing the detections in detectors 2 through 120 about a several sample range of the detections in detector 1. If detector 1 had a detection at sample 600 and the drift factor was plus or minus 10 samples, then samples 590 to 610 in the other channels were searched for detections.

As an example of channel-to-channel false alarm reduction, all the detections in channel 1 of longwave scene 0157-01 were saved and then compared to consecutive channels. Using an LLSF sample size of 40 and a range of plus/minus 10 samples, the detections were compared until at channel 9 only the horizon detection, sample 660, remained. Figures 7 and 8 (scene 0157-01, channel 21) show what a typical channel in this scene looks like. The results were different when tried on the same scene in the midwave (Figure 17). The horizon detection sample (sample 658) was lost at channel 79, while the horizontal wires at sample 632 were still producing a detection. If the detections produced by the wire had been ignored, the horizon would have been the last remaining detection at channel 27.

The second method for detecting the horizon was based on the same reasoning that is used when a sample is determined qualitatively (chosen by eye). In general, the sky radiance has a lower standard deviation than the sea radiance. In a graph such as Figure 8, a line following the sky will predict where the next several samples should lie. If those points are very different than the predicted value, it is likely an edge is present. If it is a sharp edge, then at some point the samples will start to be a large distance away from the predicted value. This is the basis for what will be called the prediction method and is depicted in Figure 22. The horizon area is first narrowed to 100-200 samples using the zero-crossing method. Starting at the sky side of this range, a 40 sample LLSF can be made, the standard deviation of the actual data and the LLSF can be calculated, and the next sample as predicted by the LLSF can be compared with the actual data sample. The number

of standard deviations the actual data is away from the predicted value can be stored and the whole process repeated for each 40 samples of the 100-200 sample range. In the event of an edge, the difference between the predicted radiance and the actual radiance will increase noticeably.

As an example, the prediction method was used on one scan of the longwave and midwave scenes of 0157-01 (Figures 8 and 18). The left side of Table 4 shows the longwave, prediction method results for samples 650-670. The first column is the sample in channel 21 whose value is being compared to the predicted value. The second column is a measure of the variance of the actual data about the LLSF. It is the standard deviation of the difference between each point in the LLSF and the actual data. The third column takes the difference between the predicted sample value and the data sample value and divides it by the standard deviation of column two. It is the number of standard deviation units from the data sample to the predicted sample. A positive value indicates the actual data sample had a radiance lower than the predicted radiance. As expected, at sample 660 the standard deviation multiple (or ratio) has increased greatly indicating the horizon drop in radiance has started.

The right side of Table 4 shows the results of the same process on the midwave (scene 0157-01). Only a small increase in the standard deviation multiple at around sample 659 (due to the horizon) and at sample 653 was produced. The absence of an increasing ratio over several samples emphasizes that this is a low contrast horizon and the horizon can not be detected to within two samples with confidence.

SECTION 7

CONTRAST MEASUREMENT

The zero-crossing and prediction methods help to identify the horizon area but what is needed is a quantitative measure of how the horizon contrast changes from scene to scene. Obviously the horizon contrast increases as the radiance difference between the sea and sky increases. What is not so obvious is between what starting and ending samples the radiance difference should be measured. A sample range too small may not fully reflect the total drop between the sky and sea, while a range too large may start to include the peaks and edges of other objects. Referring to Figure 8, the radiance difference calculated between samples 655 and 660 will not include the rest of the drop to the sea. However, choosing a longer range starting at sample 550 will include jumps in radiance due to water structure.

For this report a range of 50 samples (about 3.5 milliradians), starting from the first sky sample and extending 49 samples into the water, was chosen as a good angular distance for scenes with vertical scanning. This translates into 15 detectors for horizontal scanning scenes. A distance of 3.5 milliradians was enough to always be beyond the horizontal wires and into the water, and it was short enough to avoid the large water structure variations at larger distances. A precaution was also taken to prevent the 50th sample from having a standard deviation too far away from its immediate neighbors. An LLSF was applied to the 50 samples and the radiance of the last sample on the LLSF line was taken. This reduced the effect of water structure edges on the horizon contrast. Typically, however, the difference between the 50th sample of the actual data and the 50th point on the LLSF was less than 1%. Channel 21 was chosen for all vertical scenes because it avoided the oil rig and the island obstructions that were sometimes present in channels 60-120.

The procedure to measure the horizon contrast used the prediction method to find the last sample in the water before the horizon. An LLSF was taken from the first sky sample (last water sample plus one) to the 50th previous sample. The contrast radiance was then the radiance of the first sky sample minus the radiance of the 50th sample on the LLSF line. If the scene was too quantized to pick a single sample at which the horizon started, then a five scan average along with the zero-crossing method were used to pick the last water sample.

Table 5 summarizes the results of using the above procedure on both the midwave and longwave scenes. An asterisk in the radiance contrast column indicates a five scan average was done before the radiance difference was calculated. Explanations for the different contrasts will be discussed in Section 8 of this report.

One qualitative method was also used to measure the horizon contrast. Instead of measuring the radiance contrast, the sample contrast was found. This was a count of the number of samples needed to ensure the transition from sea to sky occurred. The number of samples was found by observing the channel plots and determining which samples marked the beginning and ending of the possible horizon area. The measurement is rough but does succeed in making a broad estimate of the horizon contrast which can be compared with the radiance contrast. Table 5 has the sample contrast values for all scenes and both bands. Because the measurement is subjective, not too much weight should be put on small sample contrast differences. There is little difference between a sample contrast of 2 and a contrast of 5. Noticeable changes in the contrast are realistically groups of 5, for example, 2-5 samples, 6-10 samples, 11-15, etc.

Some interesting scatter plots can be made by graphing the sample contrast versus the radiance contrast. Figure 23 is a plot of the longwave scenes. The x-axis is the radiance contrast, and the y-axis is the sample contrast. All values were taken from Table 5. Different symbols have been used to distinguish Port Hueneme from Marathon. For a radiance contrast below 1.0 W m^{-2} sr^{-1}, the sample contrast typically increases; however, there are both Port Hueneme and Marathon scenes which retain a sample contrast of two samples even below a radiance contrast of 1.0 W m^{-2} sr^{-1}.

Figure 24 is the midwave analog to Figure 23. Again, as expected, the sample contrast rises with decreasing radiance contrast. The rise begins below a radiance of about 0.05 W m^{-2} sr^{-1}, but again there are some low sample contrast values below this. In general, if a midwave scene has a low contrast horizon (contrast radiance below 0.05 W m^{-2} sr^{-1}), then a sample contrast of five or more samples will be needed to detect the horizon with confidence.

SECTION 8

ANALYSIS OF CONTRAST

The previous sections have described techniques for detecting the horizon and measuring its contrast. This section attempts to explain the differences in contrast using the available meteorological and geographical data. The explanations require a knowledge of the possible IR sources contributing to the radiance at the sensor. The greatest influence is the atmosphere between the sensor and the target. The transmittance of the atmosphere is a function of path length and particle distribution. For a long enough path length, the atmosphere begins to have a radiance equivalent to a blackbody radiating at ambient temperature. The background IR sources in this case are the water and the atmosphere. For the depression angles used in this report (-2.5 to 2.5 degrees), the water will mostly reflect the sky and IR sources in the sky (like clouds) and will partially emit at the water temperature. The water radiance can be completely blocked if the transmission of the atmosphere is low enough, or the water radiance may be small as compared to the reflected radiance of a cloud. Above the horizon the source of radiation is the atmosphere, clouds, and solar scattering effects. The radiance from the atmosphere depends on the elevation angle and the path length. The radiance decreases with increasing elevation angle because the density of the air decreases more rapidly with increasing elevation angles. The longest atmospheric path length and the most dense atmospheric path occur for small angles (100 microradians) above the horizon.

Table 6 incorporates many of the factors which may affect either the sea or sky radiance and groups them with the analyzed scenes. It is useful to determine which days had the best visibility and therefore should have had the best horizon contrast. An "NA" in a column means the data for that time was not available. The sun position was included so sun glint and solar scattering effects could be checked. A "Y" for yes was put in the clouds column if clouds were sighted over the water. This includes cumulus, cirrus, and stratus clouds as well as complete overcasts. Numerous days had temperature inversions, and this column was added to see if this had any affect on the contrast. The weather measurements, since they could not be taken at all places at all times, can only represent the field site area and not the exact path the sensor was looking through. The extinction coefficients seemed especially variable with time, so only those coefficients whose measurements were within plus or minus 3 hours of the time of the scene were used. The absolute humidity and air/water temperature difference were much more constant with time, and one sampling could be used as representative of the whole day. The air/water temperature differences at Port Hueneme were taken from a waverider buoy that collected a water temperature and an air temperature. Because the air temperature was measured close to the surface of the water, the air/water temperature difference remained fairly stable. At

Marathon the water and air temperatures collected by Dr. Jensen in the plane were used in the calculation of the air/water temperature difference. The air temperature measured on the rooftop by the sensor varied much more than the air temperature measured by the buoy. The data in the air temperature column is from the rooftop measurements at Port Hueneme and from Dr. Jensen at Marathon. Only measurements made within 1.5 hours of the time of the scene were used in the air temperature column.

Several differences between the two test sites can be seen in Table 6. The majority of Port Hueneme scenes were taken in the afternoon, while most of the Marathon scenes were taken in the morning. The Marathon scenes are scenes 0186-01 through 0200-24. The extinction coefficients for Port Hueneme are an order of magnitude higher than those for Marathon, while the Port Hueneme absolute humidity is 10 g m^{-3} less than the absolute humidity for Marathon. Typically, a higher absolute humidity would increase the extinction coefficient. The apparent contradiction may be caused by the instrument used to measure the aerosol size distribution. All the extinction coefficients in this report where calculated by Dr. Doug Jensen from particle size measurements made from the plane used at both sites. Dr. Jensen has suggested that, because the instrument he uses to measure particle size has a lower limit of 0.3 microns, particles with diameters below the limit will not affect his calculation of the extinction coefficient. If the east coast has particle distributions of smaller sizes than the west coast and if the east coast particle sizes fall below the 0.3 micron limit, it might cause the extinction coefficients to be lower for Marathon despite the higher humidity. Therefore, the extinction coefficients from a specific site can be compared, but no coefficient comparison will be made between sites.

Table 7 combines the meteorological data with the radiance contrast. The midwave contrast is in order from the maximum positive contrast to the minimum negative contrast. Immediately obvious is the separation between the two field sites. Except for 0186-1, 0198-12, and 0200-24, they are almost completely isolated. The longer atmospheric path length due to the different sensor heights and the higher absolute humidity are the major factors for the separation. The other major factor in the ordering of the contrast seems to be solar scattering. This factor gave the greatest contrast at a time of about 1800 at the 240 degree sensor azimuth; after 1800 the sun set and the contrast decreased rapidly as is evident in scenes 0163-55, 0163-64, and 0163-61. If the afternoon Port Hueneme scenes which had the same time but azimuths of 222 and 240 degrees are compared, the scenes with azimuths of 240 degrees had a higher positive contrast because of the scattering. For day 0165 the low Port Hueneme extinction coefficient may have contributed to it being ranked at the top of the list despite the smaller azimuths. The large negative contrast of scene 0200-24 was due to severe sun glint (see Figure 9). It is not obvious if the air/water temperature difference, temperature inversion, or clouds affected the contrast although the cloud scenes did tend to clump towards the lower contrasts.

Table 8 is the same as Table 7 except it is the longwave radiance contrast has been ordered from the maximum positive contrast to the minimum negative contrast. Since the longwave is much less susceptible to solar effects, the order of the scenes in the list is quite different except that the path length and absolute humidity still separate the two sites. The

extinction coefficients and the clouds are more important now. With an extinction coefficient of 0.30, day 0164 would be expected to have a higher contrast. However, note that all the scenes from day 0164 had clouds in them which may explain its lower contrast. The few Port Hueneme scenes scattered in with the Marathon scenes also have clouds in them. The clouds reduced the contrast but, in the absence of clouds, the extinction coefficient appears to be the greatest indicator of contrast. None of the other parameters, such as the air/water temperature difference, had a noticeable effect on the contrast.

In order to compare the contrast between the midwave and longwave, some common units need to be defined. One method is to relate the radiance contrast to the NEI of the sensor. If all the radiance contrast values were expressed as irradiance and divided by the NEI, then a measure of the contrast above the sensor noise would result. The output of this approach is listed in Table 9 for the midwave and longwave.

Another midwave/longwave contrast comparison can be done by converting the radiance contrast into the equivalent change in temperature. Since this is dependent on the initial radiance of the scene, the appropriate apparent temperature must first be chosen and then the radiance needed to produce a change of 1 degree Celsius can be found. Apparent temperatures found from the radiance around the horizon in the longwave varied from 13 to 16 degrees Celsius at Port Hueneme and 27.5 to 28.5 degrees at Marathon. In the midwave the apparent temperatures varied from 15 to 19 degrees at Port Hueneme and 28-31 degrees at Marathon. The chosen reference temperatures for calculating the radiance needed to create a 1 degree change in temperature were the midpoints of the ranges stated. The results are given in Table 9.

In Table 9, one trend seen in both comparison methods is that the longwave generally has a greater contrast than the midwave. Those midwave scenes which have a contrast greater than the longwave are mostly glint or solar scattering scenes affected by the proximity of the sun. There are three scenes to which the above did not apply; they are 0165-46, 0164-9, and 0186-1. Of these only the first scene, 0165-46, did not have a contrast so low that the difference between the midwave and the longwave was relatively small. It is not known why 0165-46 is the exception other than it was an unusually clear day.

SECTION 9

CONCLUSIONS AND RECOMMENDATIONS

This report investigated the detection and characteristics of the IR horizon using data taken at Port Hueneme, California, and Marathon, Florida, during early to mid-summer. A zero-crossing method was used to detect the horizon over relatively large areas, and a prediction method was used in conjunction with the zero-crossing output to further resolve the horizon area. Both methods are capable of detecting the horizon and horizon-like structures. Two different approaches for measuring the horizon contrast were described: the radiance contrast method and the sample contrast method. The contrast was then compared with the meteorological data available. The analysis showed a strong sun influence in the midwave for low sun elevations which greatly increased the contrast through sun glint and solar scattering. The contrast between the two test sites was determined by the difference in path lengths and absolute humidity. The longwave contrast seemed mostly dependent on the extinction coefficient and clouds. To keep the horizon detectable to within five samples typically required a radiance contrast greater than 1.0 W m^{-2} sr^{-1} in the longwave and greater than 0.05 W m^{-2} sr^{-1} in the midwave.

It should be noted the data used in this report covers only two geographic locations over short periods of time. Therefore, the results of this study should be considered preliminary and should be applied only to these locations with the given weather conditions. The analysis suggests future tests are needed to expand the horizon database, and it suggested that different seasons and locations be sought with every effort made to acquire the corresponding meteorological data. Another useful test would be night measurements where the air temperature may be less than the water temperature. This would provide more data on negative contrast and would eliminate solar scattering effects. The absolute humidities covered in this report fall around 10 g m^{-3} and 20 g m^{-3} Horizon data collected with humidities between the two values would help fill out the database. Since the sensor heights caused such a distinction between the horizon contrast of the two sites, it would be helpful if the sensor height at future test sites could be close to those used here; otherwise, the comparison of meteorological conditions may not be possible between sites. For tests at which this is not possible, such as the test being planned for Wallops Island, Virginia, the recommendation would be to take horizon data under as many different meteorological conditions as possible.

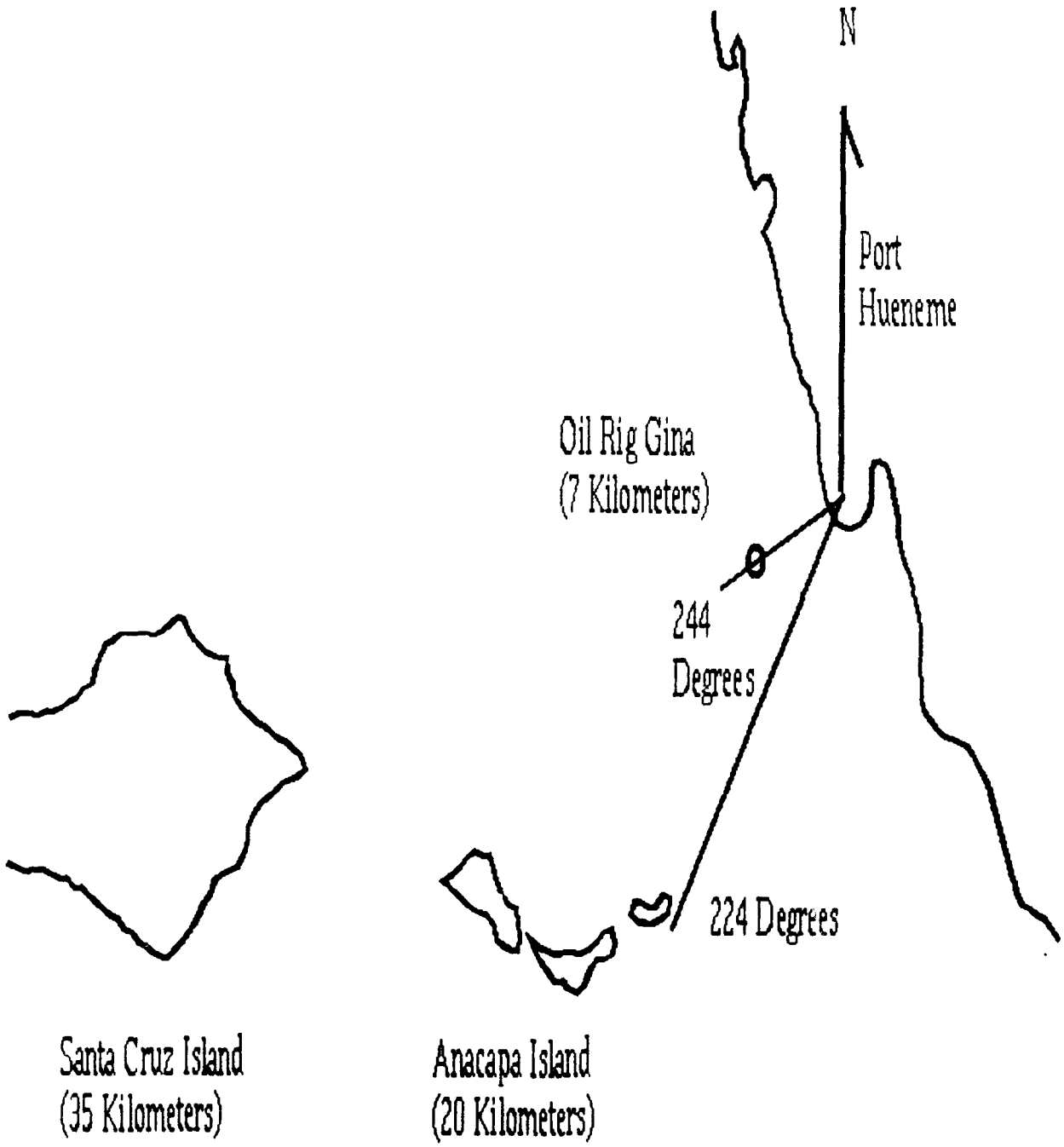

FIGURE 1. PORT HUENEME TEST SITE

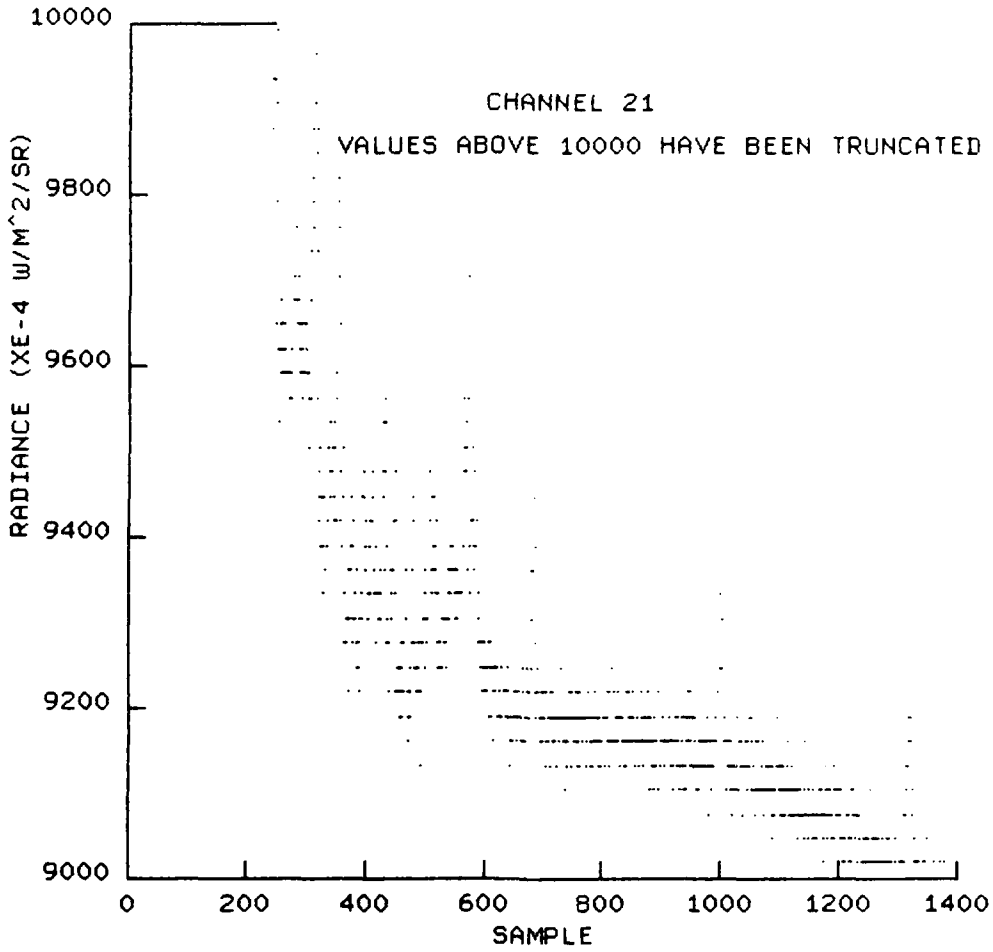

FIGURE 2. SCENE 0162-13, MIDWAVE FILTER 5

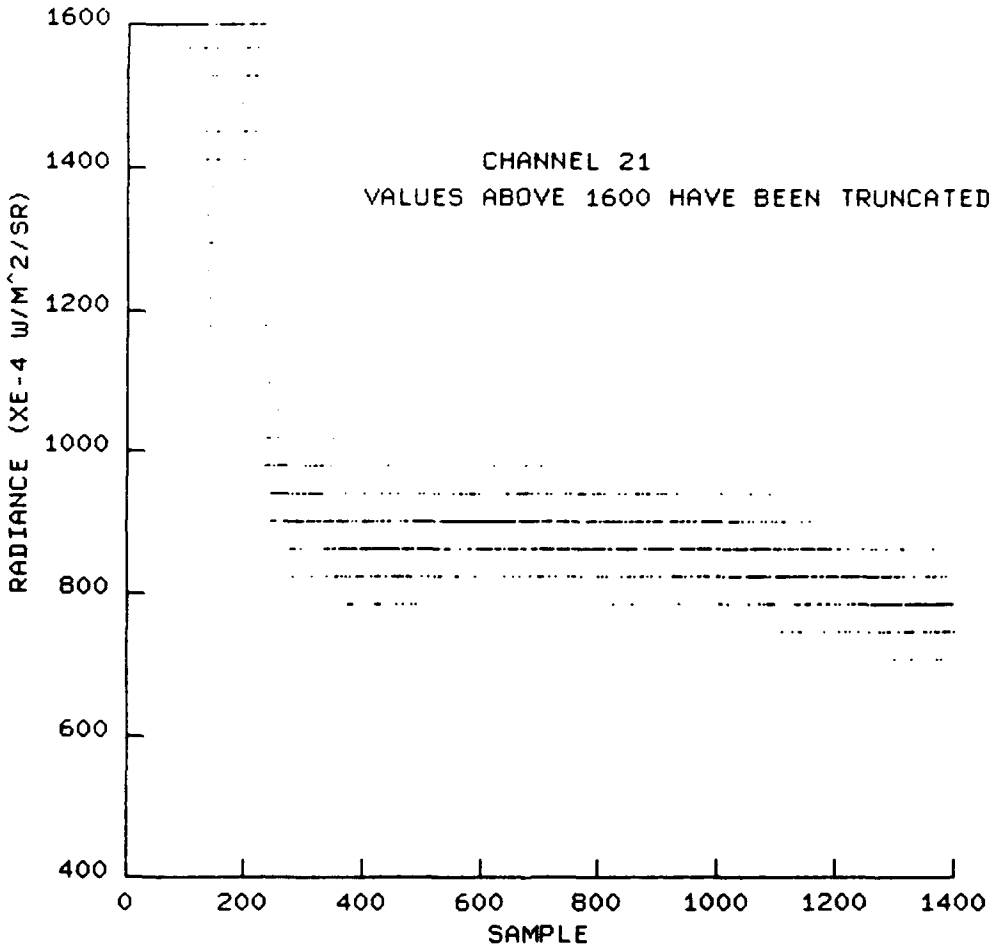

FIGURE 3. SCENE 0162-14, MIDWAVE FILTER 6

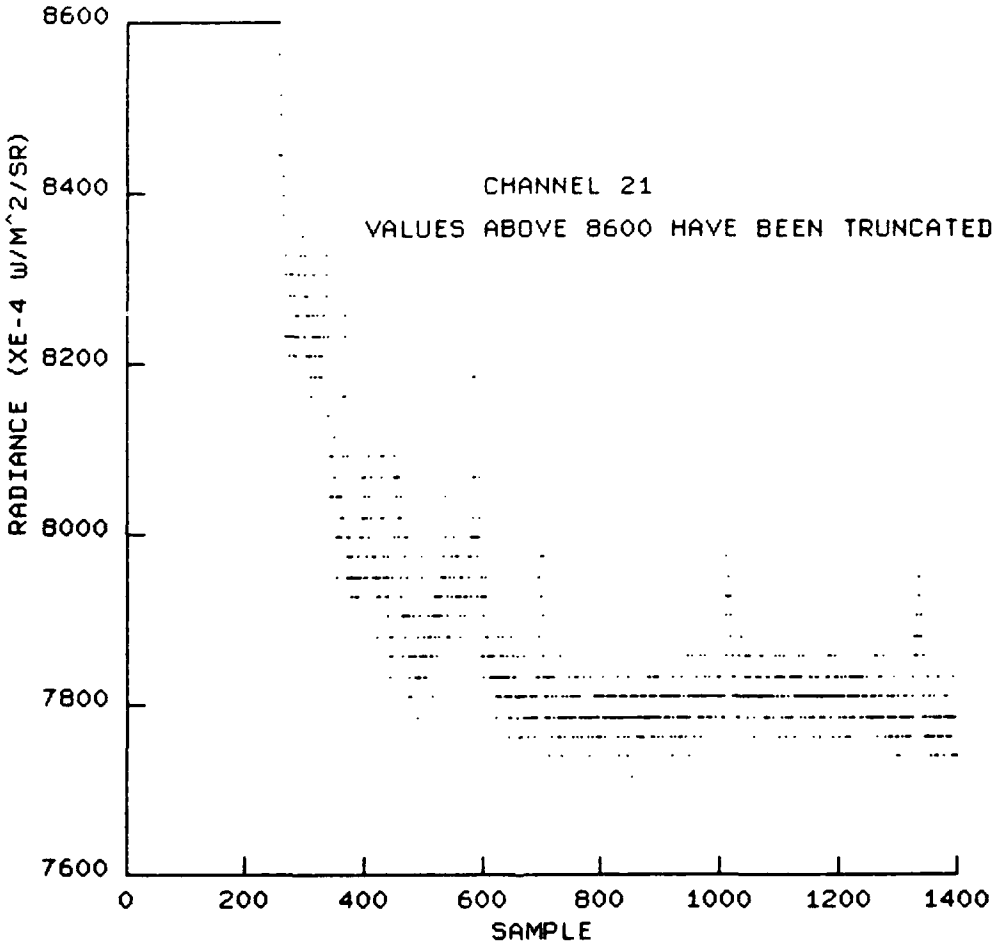

FIGURE 4. SCENE 0162-15, MIDWAVE FILTER 7

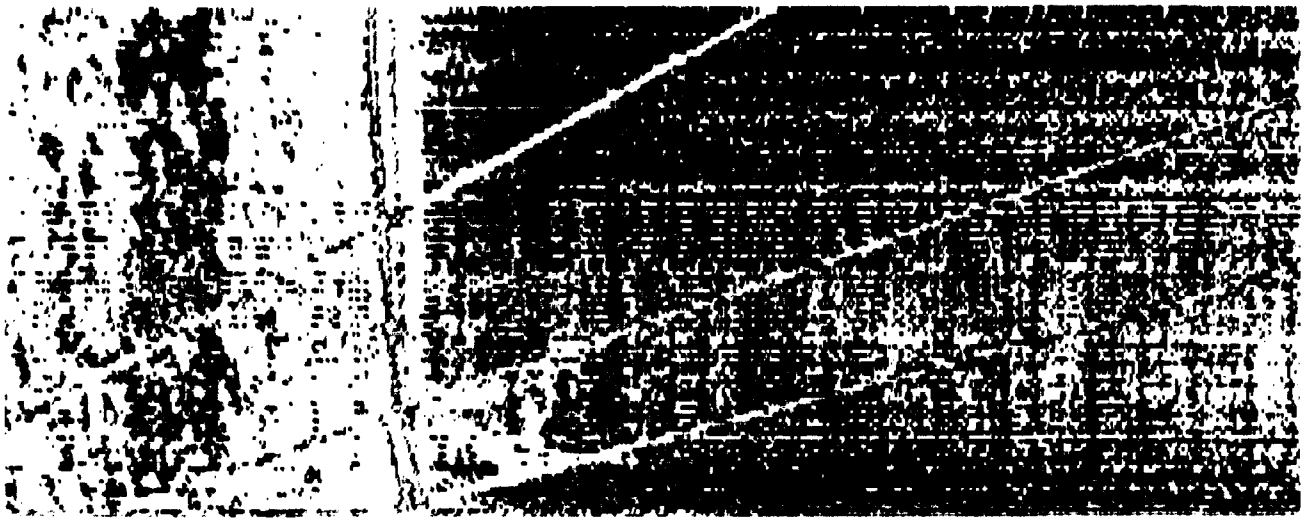

FIGURE 5. IMAGE, SCENE 0162-13, MIDWAVE FILTER 5

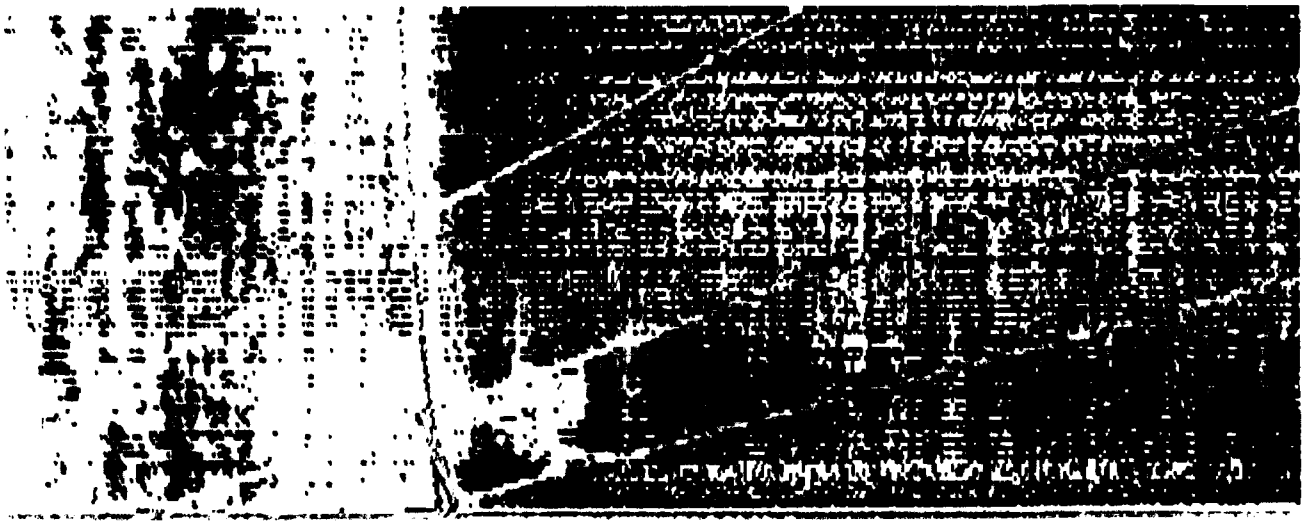

FIGURE 6. IMAGE, SCENE 0162-15, MIDWAVE FILTER 7

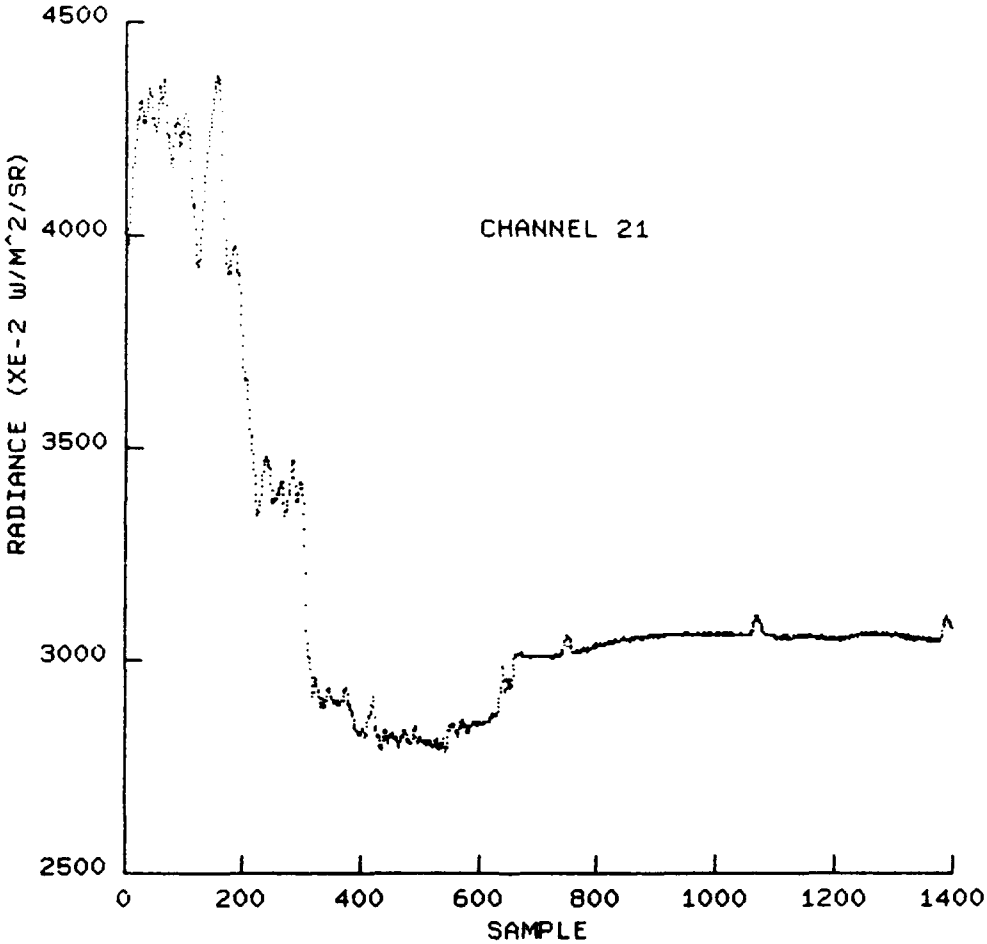

FIGURE 7. POSITIVE CONTRAST, SCENE 0157-01, LONGWAVE

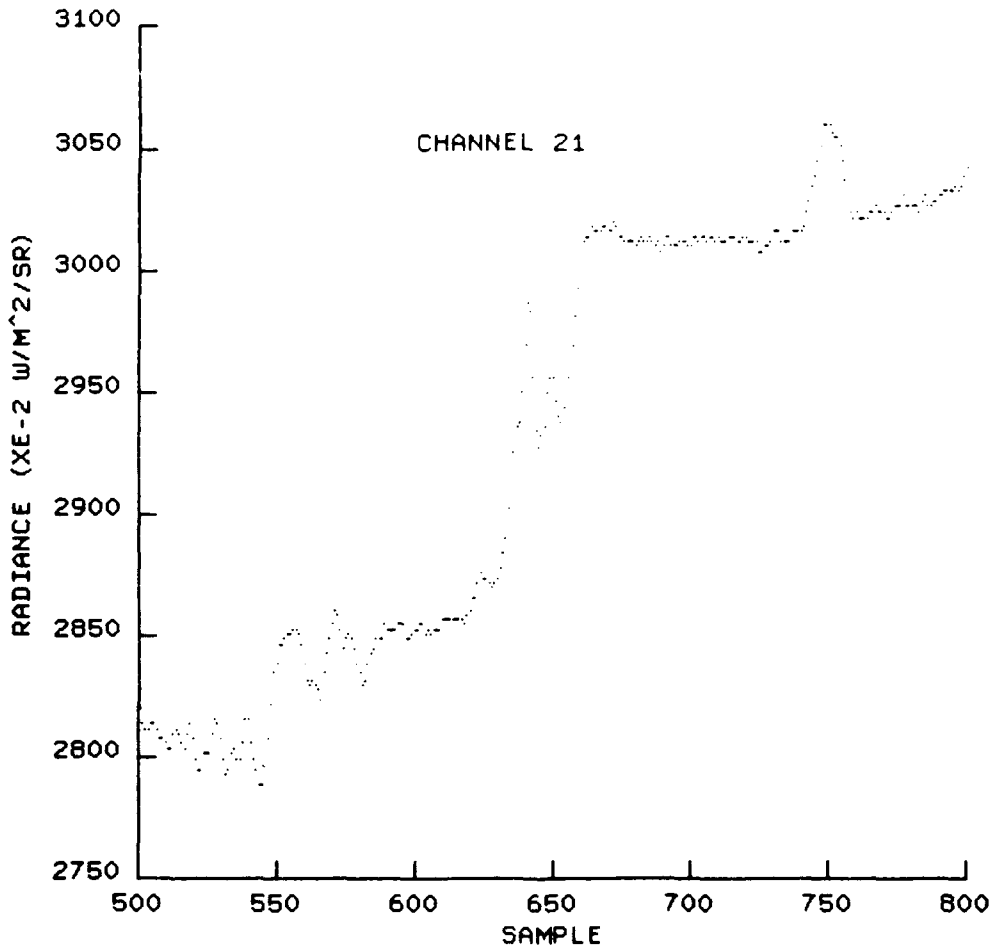

FIGURE 8. SAMPLES 500-800, SCENE 0157-01, LONGWAVE

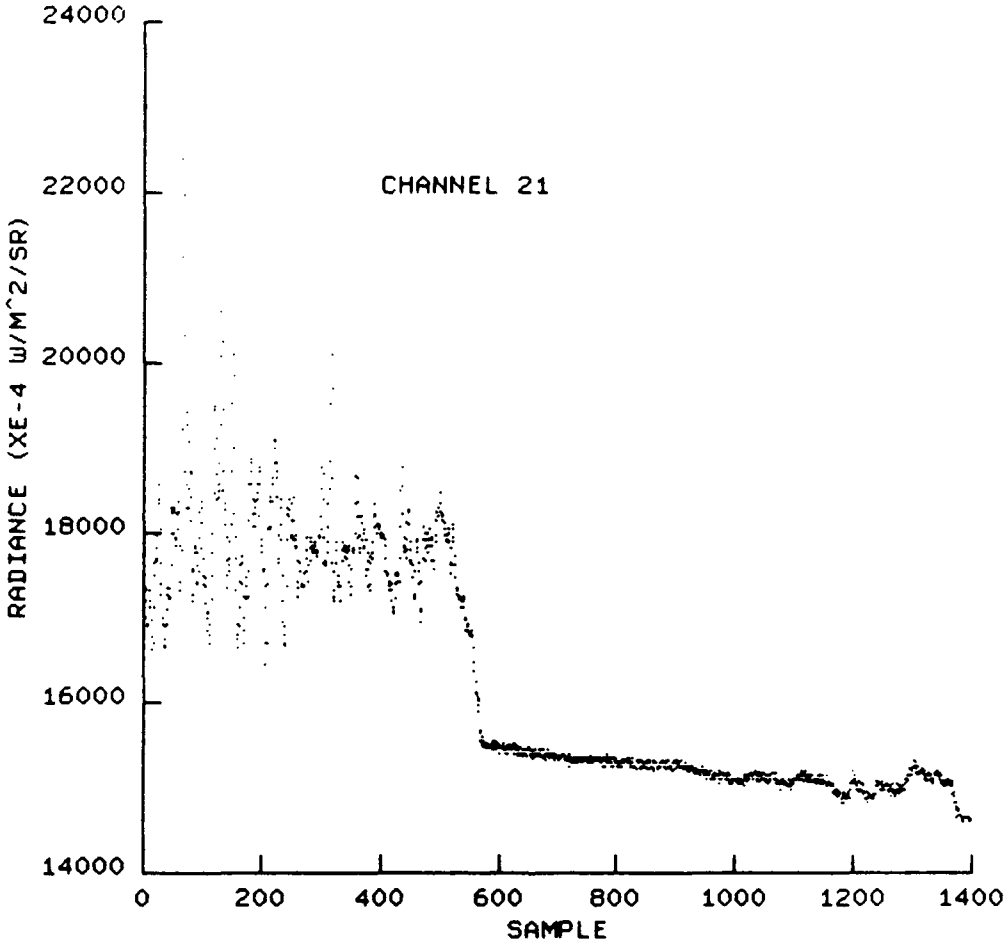

FIGURE 9. NEGATIVE CONTRAST, SCENE 0200-24, MIDWAVE

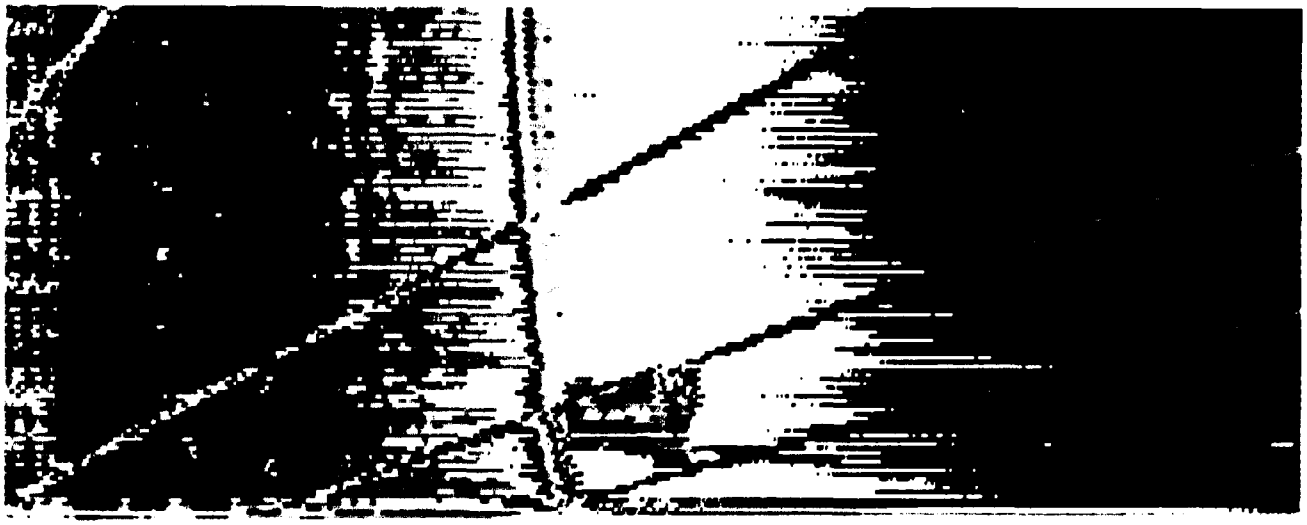

FIGURE 10. IMAGE, SCENE 0157-01, LONGWAVE

FIGURE 11. IMAGE, SCENE 0200-24, MIDWAVE

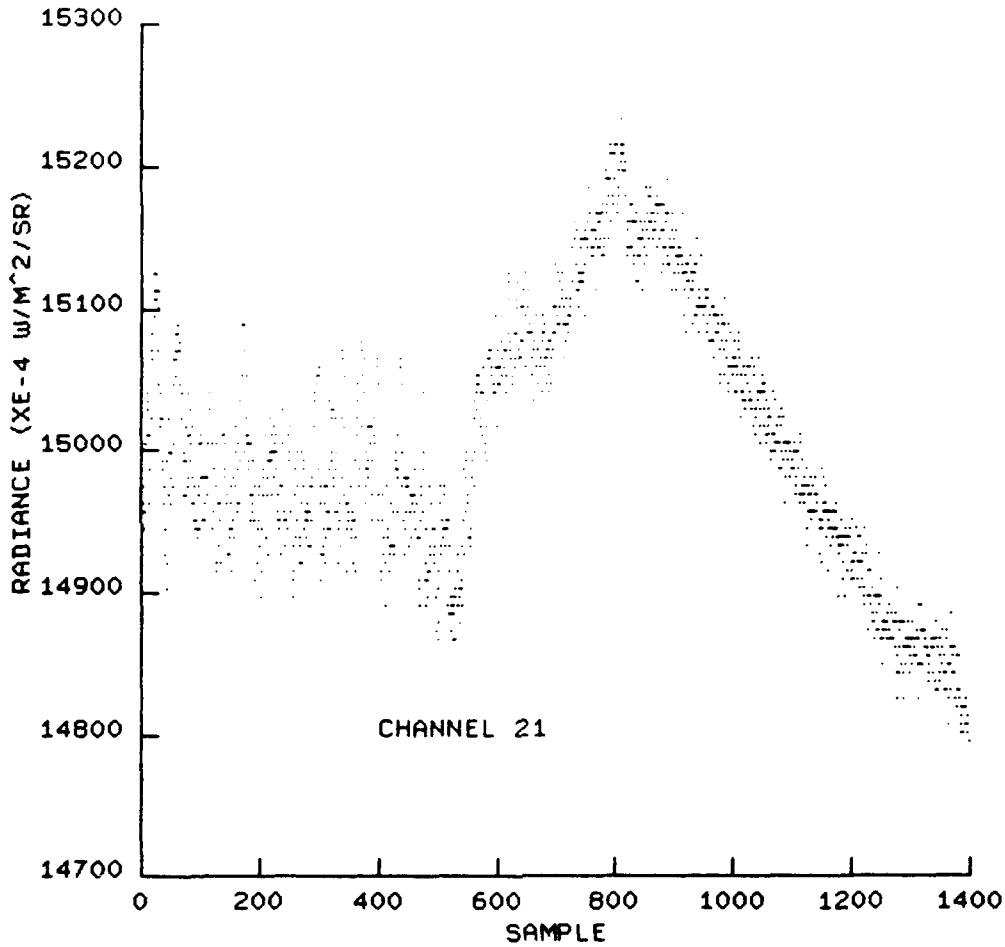

FIGURE 12. SYMMETRIC CONTRAST, 5 SCAN AVERAGE, SCENE 0195-09, MIDWAVE

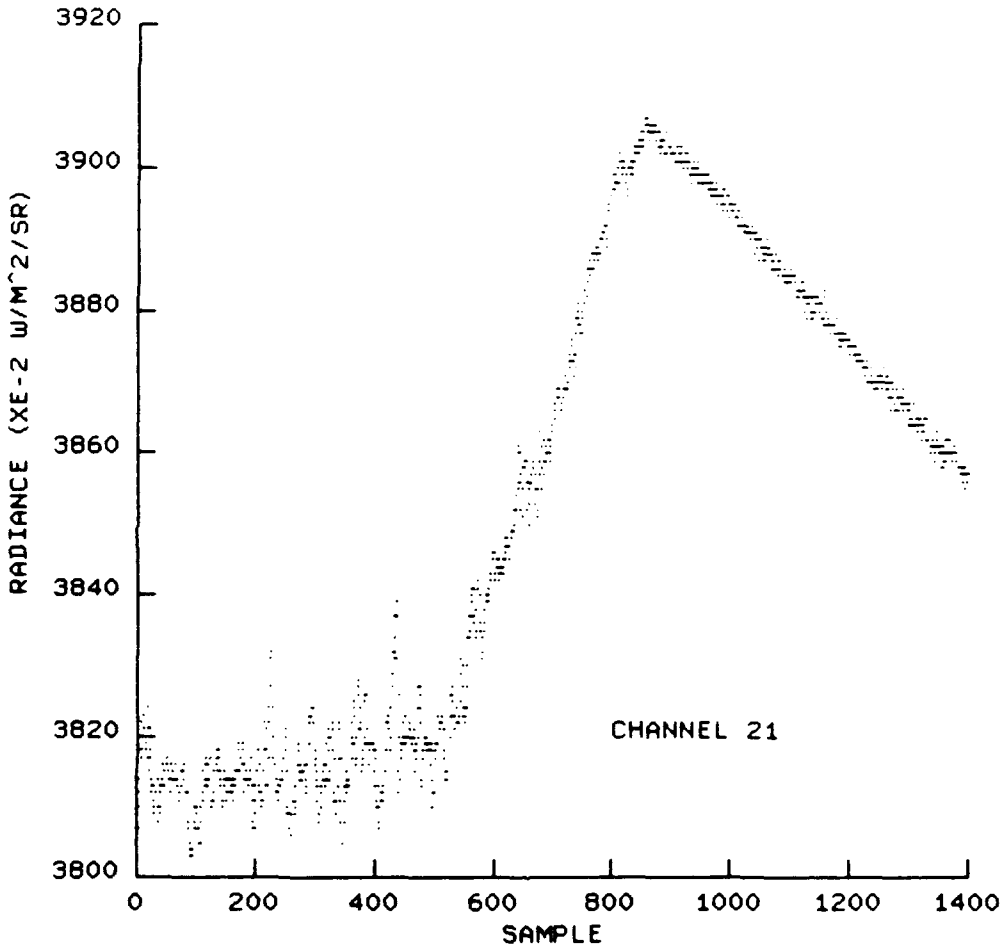

FIGURE 13. SYMMETRIC CONTRAST, 5 SCAN AVERAGE, SCENE 0195-09, LONGWAVE

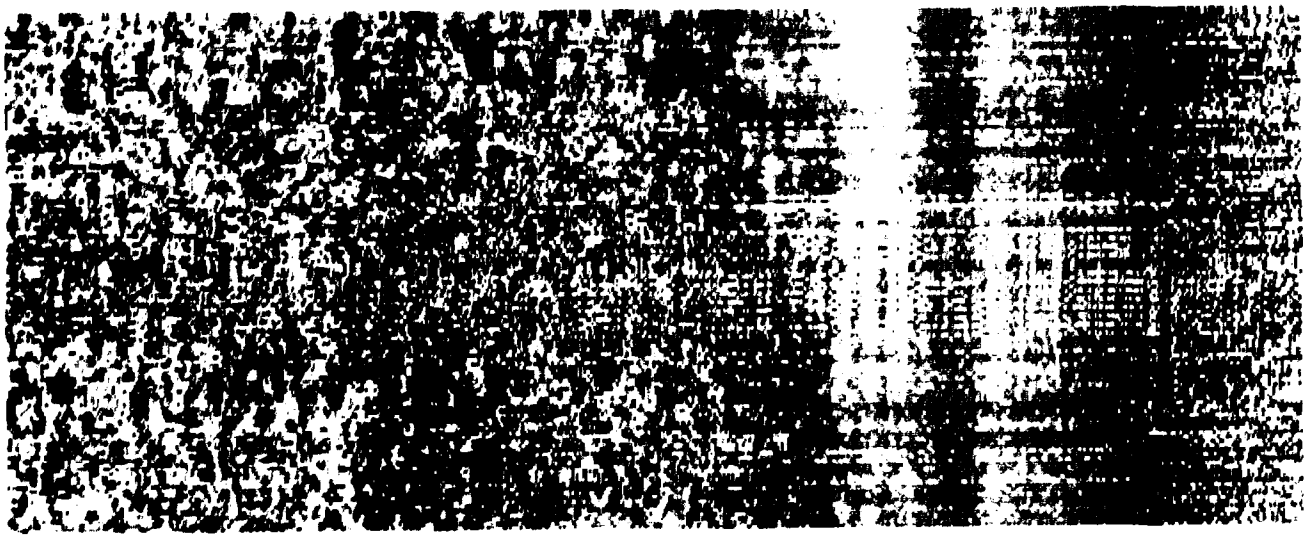

FIGURE 14. IMAGE, SCENE 0195-09, MIDWAVE, 5 SCAN AVERAGE

FIGURE 15. IMAGE, SCENE 0195-09, LONGWAVE, 5 SCAN AVERAGE

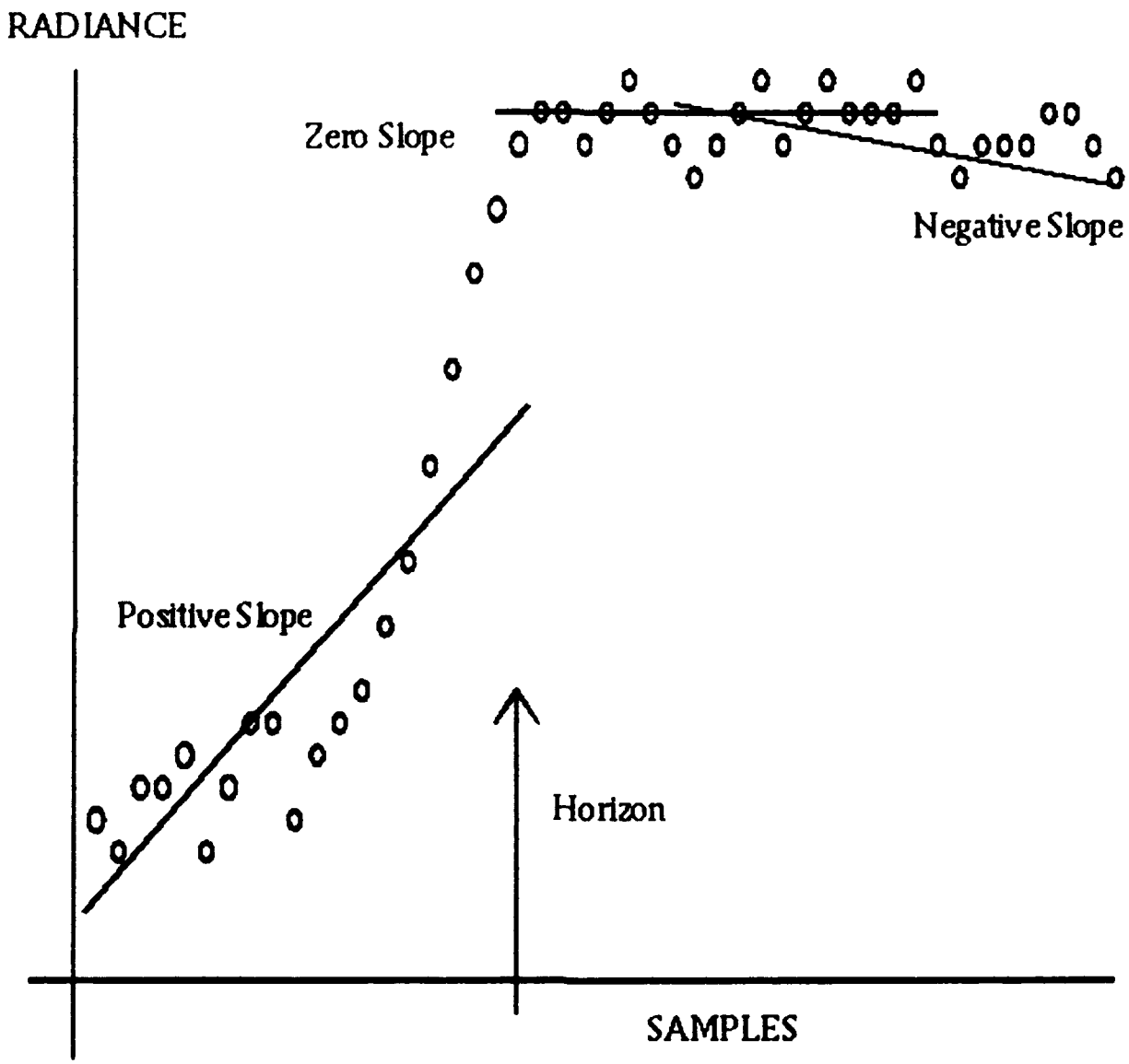

FIGURE 16. ZERO-CROSSING METHOD

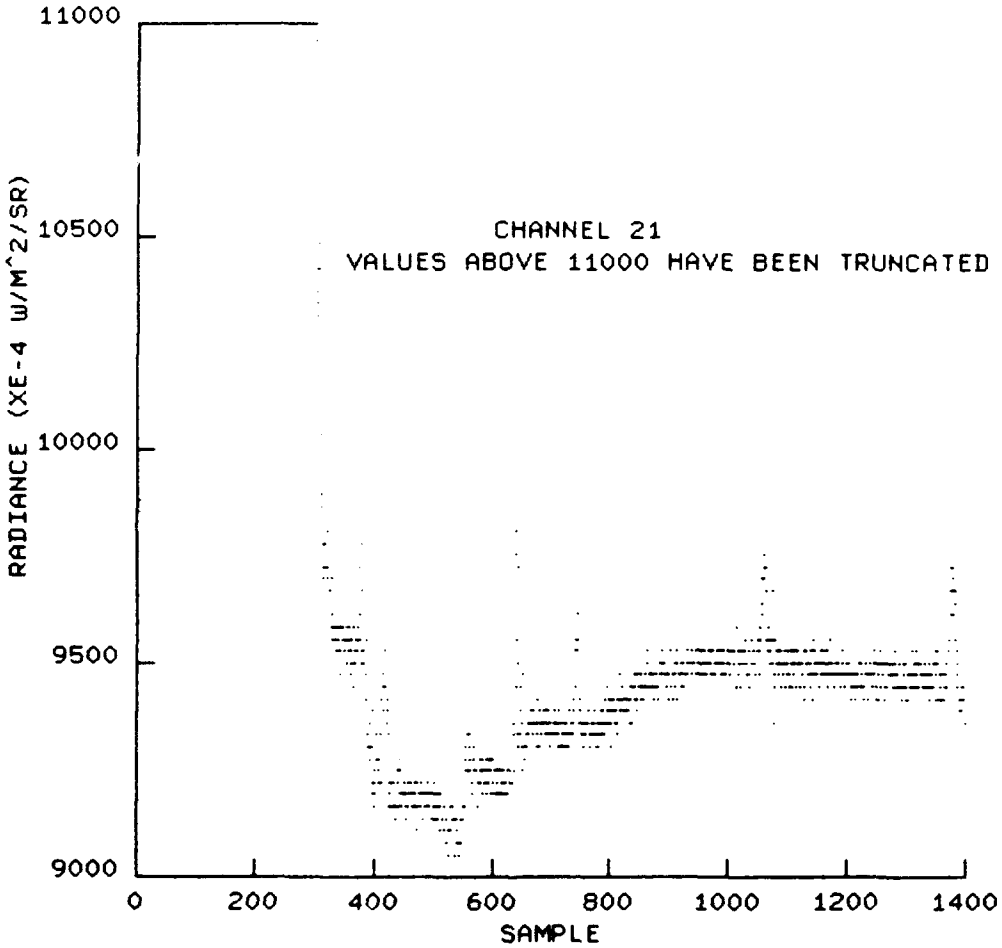

FIGURE 17. SCENE 0157-01, MIDWAVE

FIGURE 18. IMAGE, SCENE 0157-01, MIDWAVE

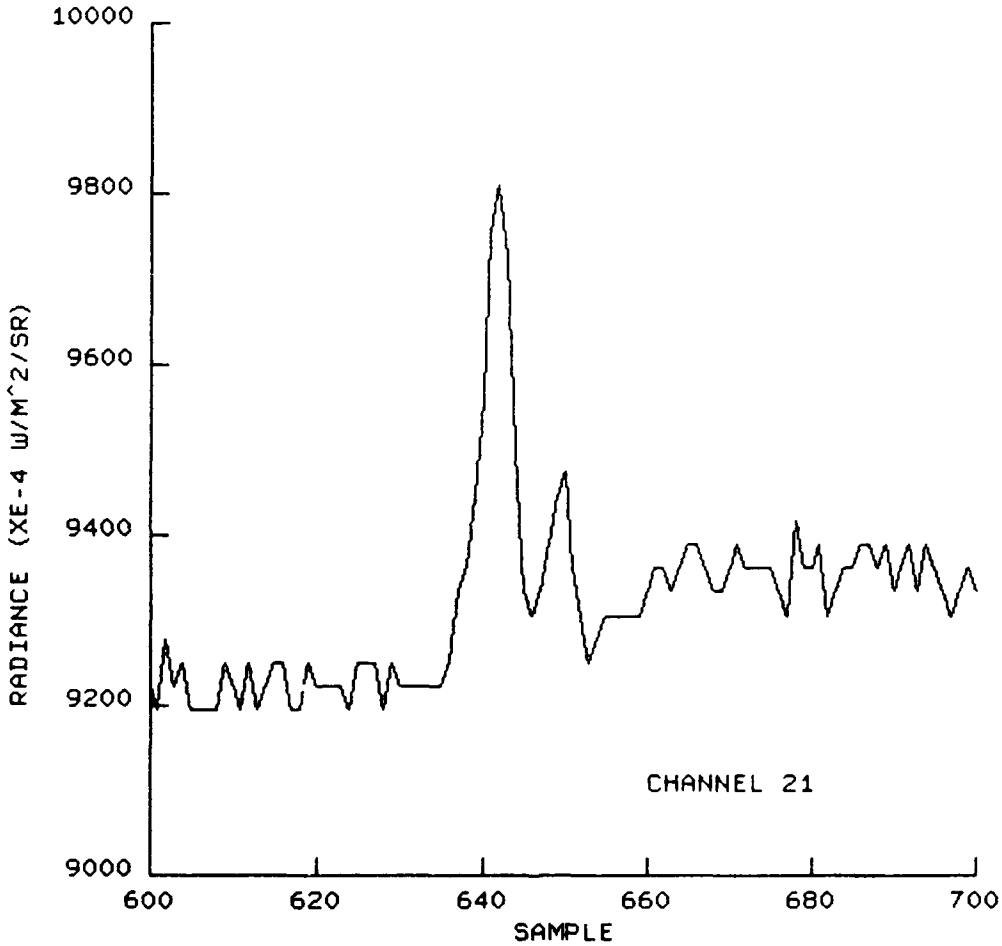

FIGURE 19. SAMPLES 600-700, SCENE 0157-01, MIDWAVE

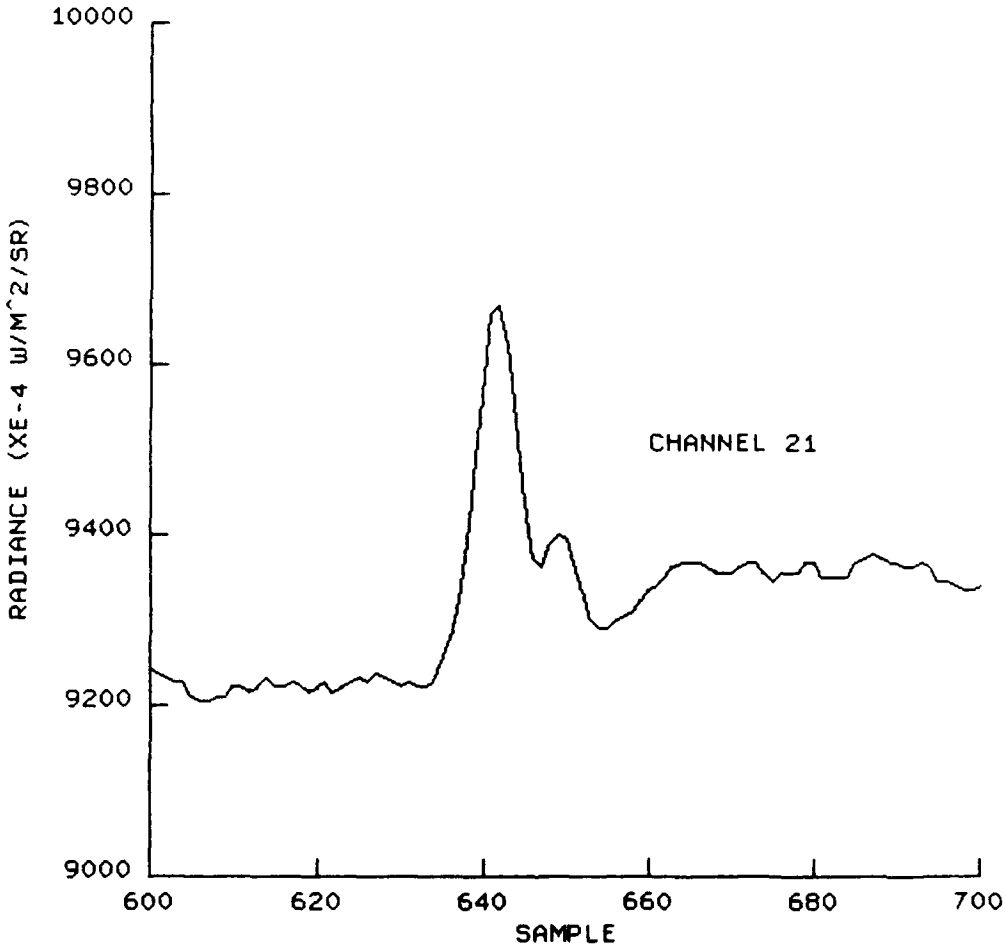

FIGURE 20. FIVE SAMPLE SMOOTHING, SAMPLES 600-700, SCENE 0157-01, MIDWAVE

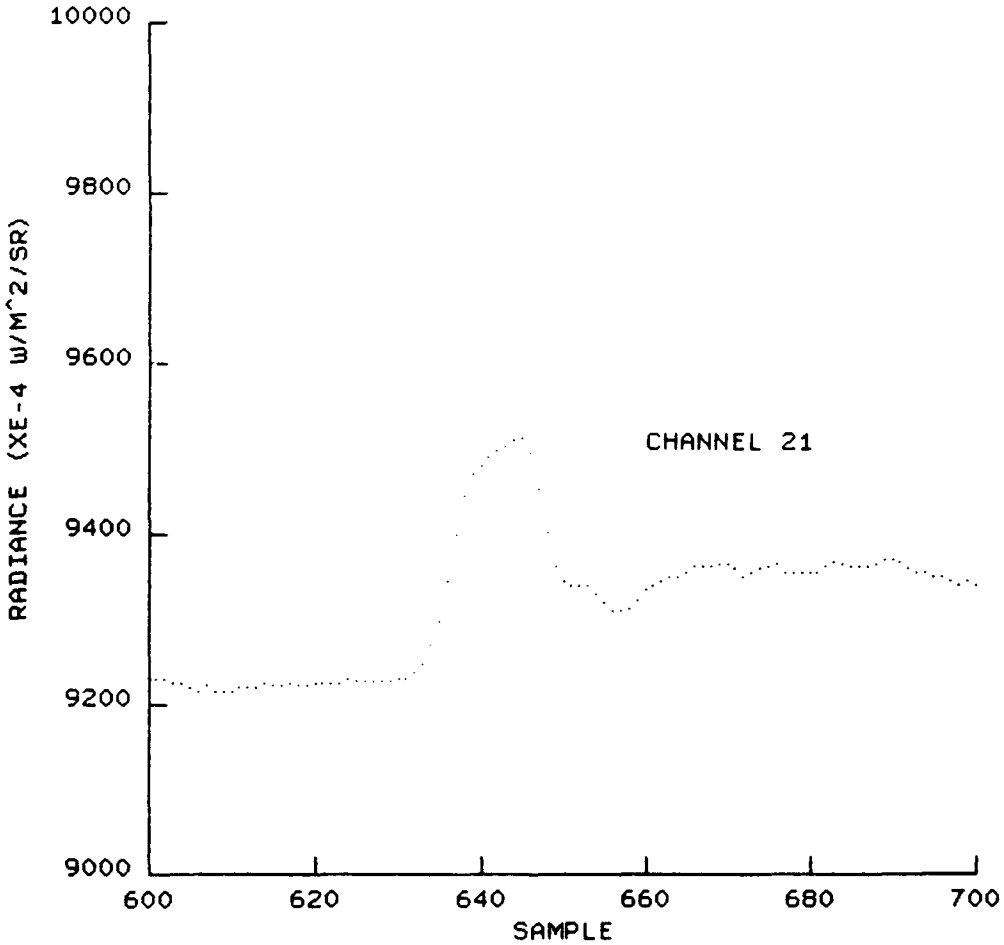

FIGURE 21. ELEVEN SAMPLE SMOOTHING, SAMPLES 600-700, SCENE 0157-01, MIDWAVE

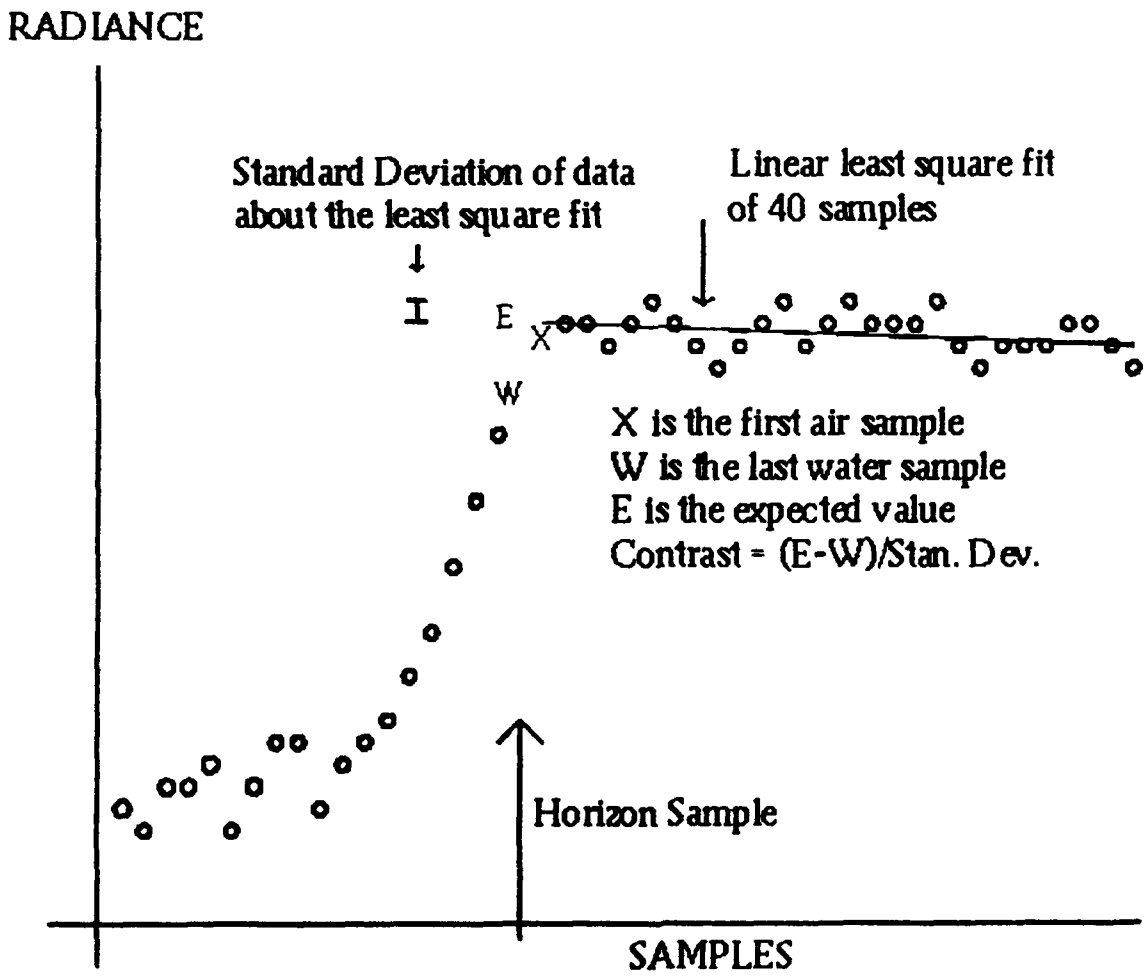

FIGURE 22. PREDICTION METHOD

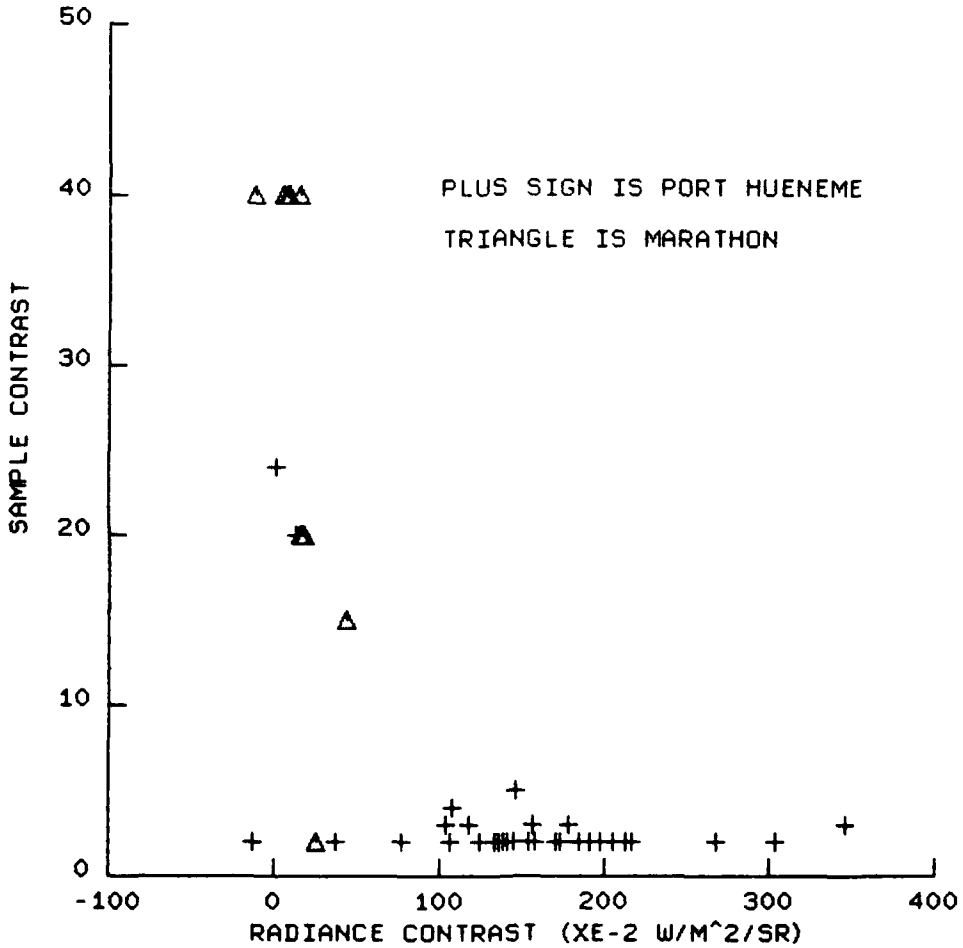

FIGURE 23. SAMPLE CONTRAST, LONGWAVE SCENES

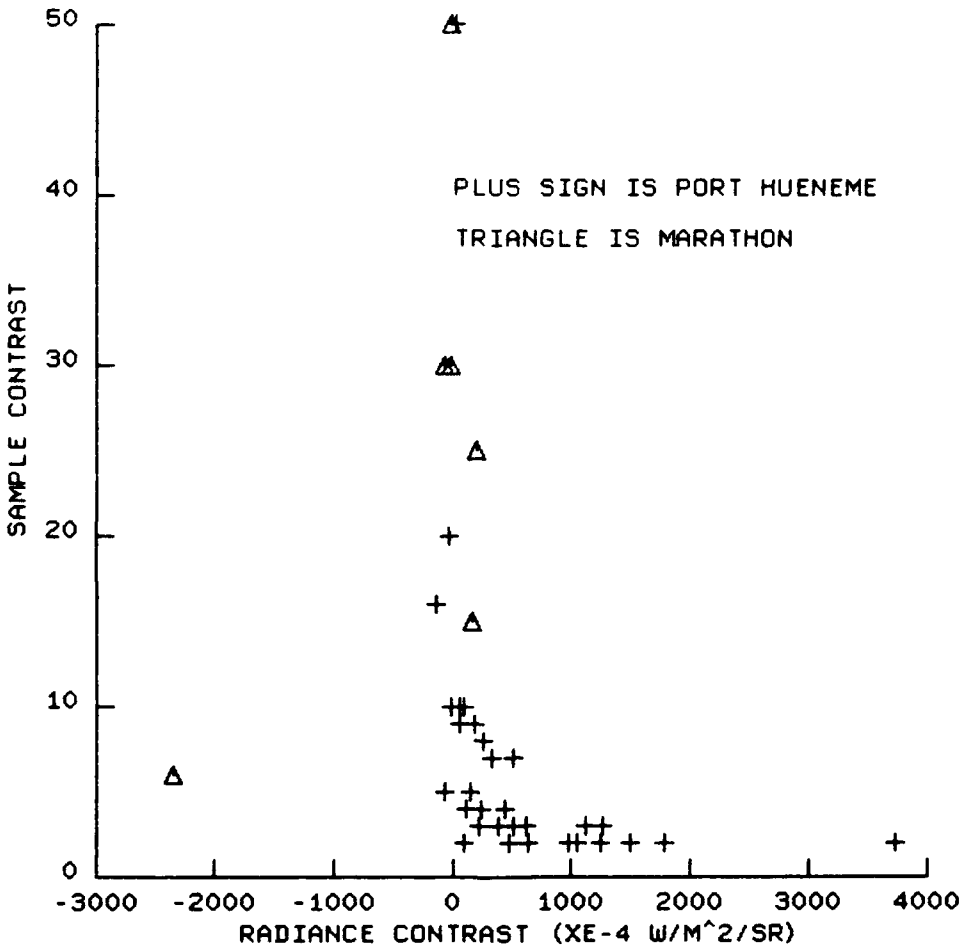

FIGURE 24. SAMPLE CONTRAST, MIDWAVE SCENES

TABLE 1. HORIZON SCENES PROCESSED

SCENE	SCANNING DIRECTION	SENSOR AZIMUTH	TIME
0152-09	HORIZONTAL	240	1352
0156-04	VERTICAL	240	1511
0156-19	VERTICAL	240	1823
0157-01	VERTICAL	240	1026
0157-10	VERTICAL	240	1322
0157-13	VERTICAL	240	1628
0158-27	VERTICAL	241	1439
0162-13	VERTICAL	240	1205
0162-19	VERTICAL	240	1300
0162-25	VERTICAL	223	1324
0162-28	VERTICAL	241	1400
0162-69	VERTICAL	241	1656
0162-72	VERTICAL	223	1701
0163-01	VERTICAL	241	0913
0163-10	VERTICAL	241	1202
0163-41	VERTICAL	241	1700
0163-49	VERTICAL	241	1800
0163-55	VERTICAL	241	1900
0163-61	VERTICAL	241	2015
0163-64	VERTICAL	241	2055
0164-03	VERTICAL	241	1038
0164-06	VERTICAL	200	1049
0164-09	VERTICAL	212	1114
0164-20	HORIZONTAL	224	1358
0164-27	HORIZONTAL	196	1526
0164-29	HORIZONTAL	222	1534
0164-31	HORIZONTAL	248	1542
0164-43	HORIZONTAL	223	1804
0165-09	HORIZONTAL	223	1302
0165-41	HORIZONTAL	301	1655
0165-46	HORIZONTAL	223	1801
0186-01	VERTICAL	149	1039
0186-12	VERTICAL	148	1134
0189-13	VERTICAL	144	0956
0195-09	VERTICAL	170	0909
0198-12	VERTICAL	170	1655
0198-13	VERTICAL	142	1808
0200-11	VERTICAL	83	0910
0200-14	VERTICAL	85	0922
0200-17	VERTICAL	91	0924
0200-22	VERTICAL	110	0929
0200-24	VERTICAL	82	1005

TABLE 2. ZERO-CROSSING, HORIZON DETECTION, SCENE 0157-01, MIDWAVE

Window Width	Total Number of Detections	Specific Detections Between Samples 600-700
20	83	602, 614, 635, 661, 678, 700
40	37	631, 660
60	18	630, 657
40 with 5 sample smoothing	24	631, 660
40 with 11 sample smoothing	19	630, 661

TABLE 3. ZERO-CROSSING DETECTION ON TEMPORALLY AVERAGED SCANS OF SCENE 0195-09

	1 scan	10 scan Average	20 scan Average	30 scan Average
Longwave Detections:				
LLSF Window width = 20	55	31	26	25
LLSF Window width = 40	24	13	14	12
Midwave Detections:				
LLSF Window width = 20	77	46	32	30
LLSF Window width = 40	32	19	18	19

TABLE 4. PREDICTION METHOD ON LONGWAVE AND MIDWAVE SCENE 0157-01

Sample Number	-----Longwave----- Standard Deviation	Ratio	-------Midwave------- Standard Deviation	Ratio
670	2.214	-1.128	25.816	0.166
669	2.211	-1.846	25.680	1.295
668	2.294	-1.562	26.096	1.147
667	2.307	-0.433	26.368	-0.053
666	2.251	-0.280	25.538	-1.054
665	2.241	-0.168	25.727	-0.895
664	2.167	-0.937	25.912	0.278
663	2.097	1.195	25.793	1.394
662	2.109	1.195	26.285	0.167
661	2.049	2.262	26.182	0.139
660	2.073	5.088	26.040	1.182
659	2.623	8.638	26.247	2.096
658	4.327	7.506	27.549	1.813
657	6.571	6.281	28.234	1.544
656	9.080	5.505	27.265	1.315
655	11.815	4.449	27.068	1.094
654	14.172	3.560	27.339	1.938
653	15.978	3.141	28.445	2.646
652	17.518	2.373	29.686	0.275
651	18.478	1.604	29.690	-1.682
650	18.842	0.775	30.524	-5.232

The ratio is the expected value minus the actual value divided by the standard deviation of the actual data about the linear least square fit.

TABLE 5. RESULTS OF RADIANCE CONTRAST AND SAMPLE CONTRAST METHODS

SCENE	AZIMUTH	TIME	Radiance Contrast ----($W\ m^{-2}\ sr^{-1}$)---- LONGWAVE ($\times 10^{-2}$)	MIDWAVE ($\times 10^{-4}$)	--SAMPLE CONTRAST-- LONGWAVE	MIDWAVE
0152-09	240	1352	303.9	475.5	2	2
0156-04	240	1511	205.5	640.8	2	2
0156-19	240	1823	191.5	1243.6	2	2
0157-01	240	1026	170.8	142.0*	2	5
0157-10	240	1322	213.4	219.7	2	3
0157-13	240	1628	217.7	967.7	2	2
0158-27	241	1439	157.8	337.8	2	7
0162-13	240	1205	77.1	-137.6*	2	16
0162-19	240	1300	119.0	-36.7*	3	20
0162-25	223	1324	154.4	90.3*	2	10
0162-28	241	1400	136.5	106.3*	2	4
0162-69	241	1656	107.6	1044.6	2	2
0162-72	223	1701	141.2	513.8	2	3
0163-01	241	0913	268.3	251.2	2	8
0163-10	241	1202	197.7	187.9	2	9
0163-41	241	1700	104.5	1121.2	3	3
0163-49	241	1800	133.7	1261.7	2	3
0163-55	241	1900	156.9	618.9	3	3
0163-61	241	2015	125.2	-64.8*	2	5
0163-64	241	2055	179.3	30.0	3	50
0164-03	241	1038	-12.3	-4.1*	2	10
0164-06	200	1049	13.9	67.6*	20	9
0164-09	212	1114	1.6	68.2*	24	10
0164-20	224	1358	139.6	239.6	2	4
0164-27	196	1526	146.9	383.9	5	3
0164-29	222	1534	108.5	432.0	4	4
0164-31	248	1542	145.0	500.9	2	7
0164-43	223	1804	37.4*	104.7*	2	2
0165-09	223	1302	346.4	1498.8	3	2
0165-41	301	1655	173.6	3742.6	2	2
0165-46	223	1801	185.8	1792.0	2	2
0186-01	149	1039	16.7*	200.0*	20	25
0186-12	148	1134	26.2	-12.6*	15	30
0189-13	144	0956	-10.7*	-60.1*	40	30
0195-09	170	0909	6.2*	-12.4*	40	50
0198-12	170	1655	44.6	171.3	15	15
0198-13	142	1808	19.2	NA	20	NA
0200-11	83	0910	9.0	NA	40	NA
0200-14	85	0922	8.8	NA	40	NA
0200-17	91	0924	15.5	NA	40	NA
0200-22	110	0929	16.6	NA	40	NA
0200-24	82	1005	16.4	-2335.9	20	6

NA stands for "Not Available".
An asterisk means a five scan average was used.

TABLE 6. METEOROLOGICAL CONDITIONS FOR EACH SCENE

SCENE	SENSOR AZIMUTH	TIME	SUN AZIMUTH	CLOUDS, TEMP. INVER.	LW, MW+ EXTINCTION COEFF. (KM^{-1})	ABSOL. HUMID. ($G\ M^{-3}$)	AWTD*	AIR TEMP. (C)
0152-09	240	1352	230	N, NA**	NA	11.0	NA	NA
0156-04	240	1511	258	N, Y	NA	10.7	1.3	21.1
0156-19	240	1823	285	N, Y	NA	10.7	2.0	18.9
0157-01	240	1026	99	Y, Y	NA	10.4	0.2	18.9
0157-10	240	1322	208	N, Y	0.50, 0.47	10.4	0.9	18.3
0157-13	240	1628	271	N, Y	0.50, 0.47	10.4	1.5	19.4
0158-27	241	1439	250	Y, Y	0.63, 0.59	11.2	1.6	18.9
0162-13	240	1205	131	N, Y	NA	9.8	0.8	20.0
0162-19	240	1300	183	N, Y	NA	9.8	0.8	20.6
0162-25	223	1324	210	N, Y	NA	9.8	0.8	20.6
0162-28	241	1400	235	N, Y	NA	9.8	0.8	20.6
0162-69	241	1656	275	N, Y	NA	9.8	0.7	19.4
0162-72	223	1701	275	N, Y	NA	9.8	0.7	19.4
0163-01	241	0913	87	N, Y	0.47, 0.44	10.3	0.2	20.6
0163-10	241	1202	129	N, Y	NA	10.3	0.2	22.8
0163-41	241	1700	275	N, Y	NA	10.3	0.6	19.4
0163-49	241	1800	283	N, Y	NA	10.3	0.7	16.7
0163-55	241	1900	290	N, Y	NA	10.3	0.8	16.7
0163-61	241	2015	300	N, Y	NA	10.3	0.8	15.0
0163-64	241	2055	306	N, Y	NA	10.3	0.8	15.0
0164-03	241	1038	100	Y, N	NA	8.9	-0.1	17.8
0164-06	200	1049	103	Y, N	NA	8.9	-0.1	17.8
0164-09	212	1114	109	Y, N	0.30, 0.30	8.9	-0.1	17.8
0164-20	224	1358	234	Y, N	0.30, 0.30	8.9	-0.1	19.4
0164-27	196	1526	261	Y, N	0.30, 0.30	8.9	0.2	19.4
0164-29	222	1534	263	Y, N	0.30, 0.30	8.9	0.2	19.4
0164-31	248	1542	264	Y, N	0.30, 0.30	8.9	0.2	19.4
0164-43	223	1804	283	Y, N	NA	8.9	0.2	17.8
0165-09	223	1302	185	N, N	0.10, 0.10	7.4	-0.1	22.2
0165-41	301	1655	275	N, N	NA	7.4	0.4	18.3
0165-46	223	1801	283	N, N	NA	7.4	-0.1	18.3
0186-01	149	1039	84	NA, N	0.01, 0.06	21.0	1.4	29.0
0186-12	148	1134	88	NA, N	0.01, 0.06	21.0	1.4	29.0
0189-13	144	0956	81	Y, N	0.01, 0.03	20.0	0.3	30.0
0195-09	170	0909	78	NA, N	0.01, 0.04	21.0	0.8	NA
0198-12	170	1655	276	NA, N	NA	20.0	0.5	NA
0198-13	142	1808	282	NA, N	NA	21.0	0.8	NA
0200-11	83	0910	79	NA, N	0.004, 0.01	19.5	0.0	NA
0200-14	85	0922	80	NA, N	0.004, 0.01	19.5	0.0	NA
0200-17	91	0924	80	NA, N	0.004, 0.01	19.5	0.0	NA
0200-22	110	0929	81	NA, N	0.004, 0.01	19.5	0.0	NA
0200-24	82	1005	84	NA, N	0.004, 0.01	19.5	0.0	NA

+LW and MW stand for Longwave and Midwave, respectively.
*AWTD stands for Air/Water Temperature Difference in degrees Celsius.
**NA stands for Not Available.

TABLE 7. MIDWAVE SORTED BY RADIANCE CONTRAST

SCENE	SCAN DIR.	AZ.	TIME	----LW AND MW----[1] RADIANCE CONTRAST ($W\ m^{-2}\ sr^{-1}$)[2]		SUN AZ.	CLOUDS, INVER.[3]	LW AND MW EXTINC. COEFFIC.[4]		HUMIDITY AND TEMPERATURE DIFFERENCE[5]	
0165-41	H	301	1655	173.6	3742.6	275	N, N	NA		7.4	0.4
0165-46	H	223	1801	185.8	1792.0	283	N, N	NA		7.4	-0.1
0165-09	H	223	1302	346.4	1498.8	185	N, N	0.10	0.10	7.4	-0.1
0163-49	V	241	1800	133.7	1261.7	283	N, Y	NA		10.3	0.7
0156-19	V	240	1823	191.5	1243.6	285	N, Y	NA		10.7	2.0
0163-41	V	241	1700	104.5	1121.2	275	N, Y	NA		10.3	0.6
0162-69	V	241	1656	107.6	1044.6	275	N, Y	NA		9.8	0.7
0157-13	V	240	1628	217.7	967.7	271	N, Y	0.50	0.47	10.4	1.5
0156-04	V	240	1511	205.5	640.8	258	N, Y	NA		10.7	1.3
0163-55	V	241	1900	156.9	618.9	290	N, Y	NA		10.3	0.8
0162-72	V	223	1701	141.2	513.8	275	N, Y	NA		9.8	0.7
0164-31	H	248	1542	145.0	500.9	264	Y, N	0.30	0.30	8.9	0.2
0152-09	H	240	1352	303.9	475.5	230	N, NA	NA		11.0	NA
0164-29	H	222	1534	108.5	432.0	263	Y, N	0.30	0.30	8.9	0.2
0164-27	H	196	1526	146.9	383.9	261	Y, N	0.30	0.30	8.9	0.2
0158-27	V	241	1439	157.8	337.8	250	Y, Y	0.63	0.59	11.2	1.6
0163-01	V	241	0913	268.3	251.2	87	N, Y	0.47	0.44	10.3	0.2
0164-20	H	224	1358	139.6	239.6	234	Y, N	0.30	0.30	8.9	-.1
0157-10	V	240	1322	213.4	219.7	208	N, Y	0.50	0.47	10.4	0.9
0186-01(m)[6]	V	149	1039	16.7*	200.0*	84	NA, N	0.01	0.06	21.0	1.4

1 LW and MW stand for Longwave and Midwave, respectively.
2 The longwave multiplier is 10^{-2} and the midwave multiplier is 10^{-4}.
3 Inversion refers to the presence of a temperature inversion.
4 The extinction coefficient units are KM^{-1}.
5 The absolute humidity has units $G\ M^{-3}$ and the air/water temperature difference units are degrees Celsius.
6 An "m" indicates the scene is from Marathon.
7 NA means Not Available.
8 An asterisk means a five scan average was used.

TABLE 7. MIDWAVE SORTED BY RADIANCE CONTRAST (Cont.)

SCENE	SCAN DIR.	AZ.	TIME	----LW AND MW----[1] RADIANCE CONTRAST ($W\ m^{-2}\ sr^{-1}$)[2]		SUN AZ.	CLOUDS, INVER.[3]	LW AND MW EXTINC. COEFFIC.[4]	HUMIDITY AND TEMPERATURE DIFFERENCE[5]	
0163-10	V	241	1202	197.7	187.9	129	N, Y	NA	10.3	0.2
0198-12(m)	V	170	1655	44.6	171.3	276	NA, N	NA	20.0	0.5
0157-01	V	240	1026	170.8	142.0*	99	Y, Y	NA	10.4	0.2
0162-28	V	241	1400	136.5	106.3*	235	N, Y	NA	9.8	0.8
0164-43	H	223	1804	37.4*	104.7*	283	Y, N	NA	8.9	0.2
0162-25	V	223	1324	154.4	90.3*	210	N, Y	NA	9.8	0.8
0164-09	V	212	1114	1.6	68.2*	109	Y, N	0.30 0.30	8.9	-.1
0164-06	V	200	1049	13.9	67.6*	103	Y, N	NA	8.9	-.1
0163-64	V	241	2055	179.3	30.0	306	N, Y	NA	10.3	0.8
0200-11(m)	V	83	0910	9.0	NA	79	NA, N	0.004 0.01	19.5	0.0
0200-14(m)	V	85	0922	8.8	NA	80	NA, N	0.004 0.01	19.5	0.0
0198-13(m)	V	142	1808	19.2	NA	282	NA, N	NA	21.0	0.8
0200-22(m)	V	110	0929	16.6	NA	81	NA, N	0.004 0.01	19.5	0.0
0200-17(m)	V	91	0924	15.5	NA	80	NA, N	0.004 0.01	19.5	0.0
0164-03	V	241	1038	-12.3	-4.1*	100	Y, N	NA	8.9	-0.1
0195-09(m)	V	170	0909	6.2*	-12.4*	78	NA, N	0.01 0.04	21.0	0.8
0186-12(m)	V	148	1134	26.2	-12.6*	88	NA, N	0.01 0.06	21.0	1.4
0162-19	V	240	1300	119.0	-36.7*	183	N, Y	NA	9.8	0.8
0189-13(m)	V	144	0956	-10.7*	-60.1*	81	Y, N	0.01 0.03	20.0	0.3
0163-61	V	241	2015	125.2	-64.8*	300	N, Y	NA	10.3	0.8
0162-13	V	240	1205	77.1	-137.6*	131	N, Y	NA	9.8	0.8
0200-24(m)	V	82	1005	16.4	-2335.9	84	NA, N	0.004 0.01	19.5	0.0

1 LW and MW stand for Longwave and Midwave, respectively.
2 The longwave multiplier is 10^{-2} and the midwave multiplier is 10^{-4}.
3 Inversion refers to the presence of a temperature inversion.
4 The extinction coefficient units are KM^{-1}.
5 The absolute humidity has units $G\ M^{-3}$ and the air/water temperature difference units are degrees Celsius.
6 An "m" indicates the scene is from Marathon.
7 NA means Not Available.
8 An asterisk means a five scan average was used.

TABLE 8. LONGWAVE SORTED BY RADIANCE CONTRAST

SCENE	SCAN DIR.	AZ.	TIME	----LW AND MW----[1] RADIANCE CONTRAST ($W\ m^{-2}\ sr^{-1}$)[2]		SUN AZ.	CLOUDS, INVER.[3]	LW AND MW EXTINC. COEFFIC.[4]		HUMIDITY AND TEMPERATURE DIFFERENCE[5]	
0165-09	H	223	1302	346.4	1498.8	185	N, N	0.10	0.10	7.4	-0.1
0152-09	H	240	1352	303.9	475.5	230	N, NA	NA		11.0	NA
0163-01	V	241	0913	268.3	251.2	87	N, Y	0.47	0.44	10.3	0.2
0157-13	V	240	1628	217.7	967.7	271	N, Y	0.50	0.47	10.4	1.5
0157-10	V	240	1322	213.4	219.7	208	N, Y	0.50	0.47	10.4	0.9
0156-04	V	240	1511	205.5	640.8	258	N, Y	NA		10.7	1.3
0163-10	V	241	1202	197.7	187.9	129	N, Y	NA		10.3	0.2
0156-19	V	240	1823	191.5	1243.6	285	N, Y	NA		10.7	2.0
0165-46	H	223	1801	185.8	1792.0	283	N, N	NA		7.4	-0.1
0163-64	V	241	2055	179.3	30.0	306	N, Y	NA		10.3	0.8
0165-41	H	301	1655	173.6	3742.6	275	N, N	NA		7.4	0.4
0157-01	V	240	1026	170.8	142.0*	99	Y, Y	NA		10.4	0.2
0158-27	V	241	1439	157.8	337.8	250	Y, Y	0.63	0.59	11.2	1.6
0163-55	V	241	1900	156.9	618.9	290	N, Y	NA		10.3	0.8
0162-25	V	223	1324	154.4	90.3*	210	N, Y	NA		9.8	.8
0164-27	H	196	1526	146.9	383.9	261	Y, N	0.30	0.30	8.9	0.2
0164-31	H	248	1542	145.0	500.9	264	Y, N	0.30	0.30	8.9	0.2
0162-72	V	223	1701	141.2	513.8	275	N, Y	NA		9.8	0.7
0164-20	H	224	1358	139.6	239.6	234	Y, N	0.30	0.30	8.9	-0.1
0162-28	V	241	1400	136.5	106.3*	235	N, Y	NA		9.8	0.8
0163-49	V	241	1800	133.7	1261.7	283	N, Y	NA		10.3	0.7
0163-61	V	241	2015	125.2	-64.8*	300	N, Y	NA		10.3	0.8
0162-19	V	240	1300	119.0	-36.7*	183	N, Y	NA		9.8	0.8

1 LW and MW stand for Longwave and Midwave, respectively.
2 The longwave multiplier is 10^{-2} and the midwave multiplier is 10^{-4}.
3 Inversion refers to the presence of a temperature inversion.
4 The extinction coefficient units are KM^{-1}.
5 The absolute humidity has units $G\ M^{-3}$ and the air/water temperature difference units are degrees Celsius.
6 An "m" indicates the scene is from Marathon.
7 NA means Not Available.
8 An asterisk means a five scan average was used.

TABLE 8. LONGWAVE SORTED BY RADIANCE CONTRAST (Cont.)

SCENE	SCAN DIR.	AZ.	TIME	----LW AND MW----[1] RADIANCE CONTRAST ($W\ m^{-2}\ sr^{-1}$)[2]		SUN AZ.	CLOUDS, INVER.[3]	LW AND MW EXTINC. COEFFIC.[4]		HUMIDITY AND TEMPERATURE DIFFERENCE[5]	
0164-29	H	222	1534	108.5	432.0	263	Y, N	0.30	0.30	8.9	0.2
0162-69	V	241	1656	107.6	1044.6	275	N, Y	NA		9.8	0.7
0163-41	V	241	1700	104.5	1121.2	275	N, Y	NA		10.3	0.6
0162-13	V	240	1205	77.1	-137.6*	131	N, Y	NA		9.8	0.8
0198-12(m)	V	170	1655	44.6	171.3	276	NA, N	NA		20.0	0.5
0164-43	H	223	1804	37.4*	104.7*	283	Y, N	NA		8.9	0.2
0186-12(m)	V	148	1134	26.2	-12.6*	88	NA, N	0.01	0.06	21.0	1.4
0198-13(m)	V	142	1808	19.2	NA	282	NA, N	NA		21.0	0.8
0186-1(m)	V	149	1039	16.7*	200.0*	84	NA, N	0.01	0.06	21.0	1.4
0200-22(m)	V	110	0929	16.6	NA	81	NA, N	0.004	0.01	19.5	0.0
0200-24(m)	V	82	1005	16.4	-2335.9	84	NA, N	0.004	0.01	19.5	0.0
0200-17(m)	V	91	0924	15.5	NA	80	NA, N	0.004	0.01	19.5	0.0
0164-06	V	200	1049	13.9	67.6*	103	Y, N	NA		8.9	-0.1
0200-11(m)	V	83	0910	9.0	NA	79	NA, N	0.004	0.01	19.5	0.0
0200-14(m)	V	85	0922	8.8	NA	80	NA, N	0.004	0.01	19.5	0.0
0195-09(m)	V	170	0909	6.2*	-12.4*	78	NA, N	0.01	0.04	21.0	0.8
0164-09	V	212	1114	1.6	68.2*	109	Y, N	0.30	0.30	8.9	-0.1
0189-13(m)	V	144	0956	-10.7*	-60.1*	81	Y, N	0.01	0.03	20.0	0.3
0164-03	V	241	1038	-12.3	-4.1*	100	Y, N	NA		8.9	-0.1

1 LW and MW stand for Longwave and Midwave, respectively.
2 The longwave multiplier is 10^{-2} and the midwave multiplier is 10^{-4}.
3 Inversion refers to the presence of a temperature inversion.
4 The extinction coefficient units are KM^{-1}.
5 The absolute humidity has units $G\ M^{-3}$ and the air/water temperature difference units are degrees Celsius.
6 An "m" indicates the scene is from Marathon.
7 NA means Not Available.
8 An asterisk means a five scan average was used.

TABLE 9. RADIANCE CONTRAST IN NEI UNITS AND CELSIUS DEGREES

SCENE	LONGWAVE NEI UNITS	MIDWAVE NEI UNITS	LONGWAVE DEGREES C	MIDWAVE DEGREES C
0152-09	61.83	9.67	5.42	1.26
0156-04	41.81	13.03	3.66	1.70
0156-19	38.96	25.30	3.41	3.30
0157-01	34.75	02.88	3.05	0.37
0157-10	43.41	04.47	3.81	0.58
0157-13	44.29	19.68	3.88	2.57
0158-27	32.10	06.87	2.81	0.89
0162-13	15.68	-2.79	1.37	-0.36
0162-19	24.21	-0.74	2.12	-0.97
0162-25	31.41	1.83	2.75	0.24
0162-28	27.77	2.16	2.43	0.28
0162-69	21.89	21.25	1.92	2.77
0162-72	28.72	10.45	2.52	1.36
0163-01	54.58	5.11	4.79	0.66
0163-10	40.22	3.82	3.53	0.49
0163-41	21.26	22.81	1.86	2.98
0163-49	27.20	25.67	2.38	3.35
0163-55	31.92	12.59	2.80	1.64
0163-61	25.47	-1.31	2.23	-0.17
0163-64	36.48	0.61	3.20	0.07
0164-03	-2.50	-0.08	-0.21	-0.01
0164-06	2.82	1.37	0.24	0.17
0164-09	0.32	1.38	0.02	0.18
0164-20	28.40	4.87	2.49	0.63
0164-27	29.88	7.81	2.62	1.02
0164-29	22.07	8.78	1.93	1.14
0164-31	29.50	10.19	2.58	1.33
0164-43	7.60	2.13	0.66	0.27
0165-09	70.48	30.49	6.18	3.98
0165-41	35.32	76.14	3.10	9.95
0165-46	37.80	36.46	3.31	4.76
0186-01	3.39	4.06	0.25	0.36
0186-12	5.33	-0.25	0.40	-0.02
0189-13	-2.17	-1.22	-0.16	-0.11
0195-09	1.26	-0.25	0.09	-0.02
0198-12	9.07	3.48	0.69	0.31
0198-13	3.90	NA	0.29	NA
0200-11	1.83	NA	0.13	NA
0200-14	1.79	NA	0.13	NA
0200-17	3.15	NA	0.23	NA
0200-22	3.37	NA	0.25	NA
0200-24	3.33	-47.52	0.25	-4.31

NA stands for Not Available.

DISTRIBUTION

	Copies
Commanding Officer Naval Research Laboratory Attn: Code 6520 (Dr. J. Kerschenstein) 4555 Overlook Ave., S.W. Washington, DC 20375	2
Commander Naval Air Development Center Attn: Code 3011 (H. Sokoloff) Warminster, PA 18974-5000	2
Office of Naval Technology Attn: Code 214 (Jim Hall) 800 North Quincy Street Arlington, VA 22217-5000	2
Commander Naval Sea Systems Command Attn: PMS-421 (A. Cote) PMS-413.1 (J. Gamer) Washington, DC 20362-5101	 1 1
Institute of Defense Analysis Attn: Russell Fries for Dr. E. Bauer 1801 N. Beauregard Street Alexandria, VA 22331	1
ONTAR Attn: Gretchen Schroeder for Dr. J. Schroeder 129 University Road Brookline, MA 02146	1
Raytheon Company Attn: Stephen McQuiggar for Dr. J. Hobson Missile Systems Division 50 Apple Hill Drive Tewksbury, MA 01876-0901	1
Johns Hopkins University Applied Physics Laboratory Attn: Dianna Jones, Supervisor of Library Acquisition for Dr. R. Steinberg Fleet Systems Department Johns Hopkins Road Laurel, MD 20707	1
Library of Congress Attn: Gift and Exchange Division Washington, DC 20540	4
Defense Technical Information Center Cameron Station Alexandria, VA 22304-6145	12

DISTRIBUTION (Cont.)

	Copies
Internal Distribution:	
E231	2
E232	3
E342 (GIDEP)	1
F41 (D. Kirkpatrick)	1
F41 (K. Krueger)	1
F41 (R. Stapleton)	5
F41 (R. Stump)	1
F41 (R. Wiss)	1
F44 (K. Hepfer)	1
G06 (R. Staton)	1
R40 (C. Larson)	1
R43 (D. Cunningham)	1
R43 (M. Kaelberer)	5
R43 (D. Crowder)	1
R44 (J. Barnett)	3

REPORT DOCUMENTATION PAGE

Form Approved
OMB No. 0704-0188

Public reporting burden for this collection of information is estimated to average 1 hour per response, including the time for reviewing instructions, searching existing data sources, gathering and maintaining the data needed, and completing and reviewing the collection of information. Send comments regarding this burden estimate or any other aspect of this collection of information, including suggestions for reducing this burden, to Washington Headquarters Services, Directorate for Information Operations and Reports, 1215 Jefferson Davis Highway, Suite 1204, Arlington, VA 22202-4302, and to the Office of Management and Budget, Paperwork Reduction Project (0704-0188), Washington, DC 20503

1. AGENCY USE ONLY *(Leave blank)*

2. REPORT DATE
31 July 1991

3. REPORT TYPE AND DATES COVERED
Final: 1 Dec 1990 -- 31 May 1991

4. TITLE AND SUBTITLE
Infrared Horizon Detection

5. FUNDING NUMBERS
n/a

6. AUTHOR(S)
Monte S. Kaelberer

7. PERFORMING ORGANIZATION NAME(S) AND ADDRESS(ES)
Naval Surface Warfare Center
White Oak Laboratory (Code R43)
10901 New Hampshire Avenue
Silver Spring, MD 20903-5000

8. PERFORMING ORGANIZATION REPORT NUMBER
NAVSWC TR 91-460

9. SPONSORING/MONITORING AGENCY NAME(S) AND ADDRESS(ES)

10. SPONSORING/MONITORING AGENCY REPORT NUMBER

11. SUPPLEMENTARY NOTES

12a. DISTRIBUTION/AVAILABILITY STATEMENT
Approved for public release; distribution is unlimited.

12b. DISTRIBUTION CODE

13. ABSTRACT *(Maximum 200 words)*

The sea/sky interface in the 3 to 5 micron and 8 to 12 micron regions is examined in this report. The efficacy of two algorithms for delineating the optical horizon is studied using infrared data taken with the Infrared Analysis Measurement and Modeling Program (IRAMMP) sensor at Port Hueneme, California, and Marathon, Florida. Several signal processing methods are described along with the performance results of computer simulations exercising the various algorithms against the IRAMMP data. Meteorological data collected at the field sites is used to aid in explaining the varying degrees of contrast exhibited by the database.

14. SUBJECT TERMS
infrared (IR) horizon radiometer detection

15. NUMBER OF PAGES
61

16. PRICE CODE

17. SECURITY CLASSIFICATION OF REPORT	18. SECURITY CLASSIFICATION OF THIS PAGE	19. SECURITY CLASSIFICATION OF ABSTRACT	20. LIMITATION OF ABSTRACT
UNCLASSIFIED	UNCLASSIFIED	UNCLASSIFIED	UL

GENERAL INSTRUCTIONS FOR COMPLETING SF 298

The Report Documentation Page (RDP) is used in announcing and cataloging reports. It is important that this information be consistent with the rest of the report, particularly the cover and its title page. Instructions for filling in each block of the form follow. It is important to ***stay within the lines*** to meet ***optical scanning requirements***.

Block 1. Agency Use Only *(Leave blank)*.

Block 2. Report Date. Full publication date including day, month, and year, if available (e.g. 1 Jan 88). Must cite at least the year.

Block 3. Type of Report and Dates Covered. State whether report is interim, final, etc. If applicable, enter inclusive report dates (e.g. 10 Jun 87 - 30 Jun 88).

Block 4. Title and Subtitle. A title is taken from the part of the report that provides the most meaningful and complete information. When a report is prepared in more than one volume, repeat the primary title, add volume number, and include subtitle for the specific volume. On classified documents enter the title classification in parentheses.

Block 5. Funding Numbers. To include contract and grant numbers; may include program element number(s), project number(s), task number(s), and work unit number(s). Use the following labels:

C	- Contract	**PR**	- Project
G	- Grant	**TA**	- Task
PE	- Program Element	**WU**	- Work Unit Accession No.

BLOCK 6. Author(s). Name(s) of person(s) responsible for writing the report, performing the research, or credited with the content of the report. If editor or compiler, this should follow the name(s).

Block 7. Performing Organization Name(s) and Address(es). Self-explanatory.

Block 8. Performing Organization Report Number. Enter the unique alphanumeric report number(s) assigned by the organization performing the report.

Block 9. Sponsoring/Monitoring Agency Name(s) and Address(es). Self-explanatory.

Block 10. Sponsoring/Monitoring Agency Report Number. *(If Known)*

Block 11. Supplementary Notes. Enter information not included elsewhere such as: Prepared in cooperation with...; Trans. of...; To be published in.... When a report is revised, include a statement whether the new report supersedes or supplements the older report.

Block 12a. Distribution/Availability Statement. Denotes public availability or limitations. Cite any availability to the public. Enter additional limitations or special markings in all capitals (e.g. NOFORN, REL, ITAR).

- **DOD** - See DoDD 5230.24, "Distribution Statements on Technical Documents."
- **DOE** - See authorities.
- **NASA** - See Handbook NHB 2200.2
- **NTIS** - Leave blank.

Block 12b. Distribution Code.

- **DOD** - Leave blank.
- **DOE** - Enter DOE distribution categories from the Standard Distribution for Unclassified Scientific and Technical Reports.
- **NASA** - Leave blank.
- **NTIS** - Leave blank.

Block 13. Abstract. Include a brief ***(Maximum 200 words)*** factual summary of the most significant information contained in the report.

Block 14. Subject Terms. Keywords or phrases identifying major subjects in the report.

Block 15. Number of Pages. Enter the total number of pages.

Block 16. Price Code. Enter appropriate price code ***(NTIS only)***

Blocks 17.-19. Security Classifications. Self-explanatory. Enter U.S. Security Classification in accordance with U.S. Security Regulations (i.e., UNCLASSIFIED). If form contains classified information, stamp classification on the top and bottom of the page.

Block 20. Limitation of Abstract. This block must be completed to assign a limitation to the abstract. Enter either UL (unlimited) or SAR (same as report). An entry in this block is necessary if the abstract is to be limited. If blank, the abstract is assumed to be unlimited.